7-15-2004

Characterization of Novel Nitroplatinum(IV) Complexes for the Treatment of Cancer

Jeannette Lo
University of South Florida

Characterization of Novel Nitroplatinum(IV) Complexes for the Treatment of Cancer

by

Jeannette Lo

A thesis submitted in partial fulfillment
of the requirements for the degree of
Master of Science in Public Health
Department of Global Health
College of Public Health
University of South Florida

Major Professor: Heidi Kay, Ph.D.
Boo Kwa, Ph.D.
Ann DeBaldo, Ph.D.

Date of Approval:
July 15, 2004

Keywords: Cisplatin, resistance, STAT, nitric oxide, angiogenesis

DEDICATION

I dedicate this to Dr. Neil Rowland, the professor that gave me a chance and inspired my initial interest in research; to my parents, whom have instilled the values of education and diligence into me; and to Dan Dauer, who gives me purpose for everything I do.

ACKNOWLEDGEMENTS

The author would like to thank her major professor Dr. Heidi Kay for her guidance during the research and writing process, and the members of the Kay lab for their contribution in the data collection. The author would also like to recognize the Jove and Yu labs for their assistance with the EMSA assay and animal toxicity studies, Ed Haller for his efforts on x-ray analysis, Laura Pendleton for her work in the Western Blot, the Moffitt clinical labs for running toxicity profiles, and Dr. George Blanck for providing cells and advice. The author also wishes to express gratitude to Dr. Boo Kwa and Dr. Ann DeBaldo for their advice as committee members. Finally, the author would like to express her gratitude to Justin Kerr, her friend and fellow collaborator on this project, who kept her both entertained and grounded, and for his hard work during the most difficult periods of the experimentation.

TABLE OF CONTENTS

LIST OF TABLES

LIST OF FIGURES

LIST OF ABBREVIATIONS

A	adenine
ALT	alanine aminotransferase
AST	aspartate aminotransferase
BUN	blood urea nitrogen
C	Celsius
CA	California
cm	centimeter
CO_2	carbon dioxide (gas)
cps	counts per second
DAF-FM	4-amino-5-methylamino-2',7'- difluorofluorescein
dept.	department
DMEM	Dulbecco's Modified Eagle Medium
DMSO	dimethyl sulfoxide
DNA	deoxyribonucleic acid
EDAX	energy dispersive x-ray analysis
EDS	energy dispersive spectroscopy
EMSA	electrophoretic mobility shift assay
etOH	ethanol
G	guanine
h	hour
HCl	hydrochloric acid
HIF-1	hypoxic inducible factor-1
hSIE	high affinity sis-inducible element
IACUC	Institutional Animal Care and Use Committee
IC_{50}	50% inhibitory concentration
iNOS	inducuble nitric oxide synthesis
kg	kilogram
kV	kilovolts
M	molar
mg	milligram
mL	milliliter
mM	millimolar
MMR	mismatch repair
MTT	3-(4,5-dimethylthaizol-2-yl)-2,5-diphenyltetrazolium bromide
NCI	National Cancer Institute
nm	nanometer
NO	nitric oxide (gas)
NOS	nitric oxide synthesis
O_2	oxygen (gas)

OR	Oregon
P	phosphate
PBS	phosphate buffered saline
PMS	N-methyl dibenzopyrazine methyl sulfate
Pt	platinum
RNA	ribonucleic acid
S phase	synthesis phase
SDS-PAGE	sodium dodecyl sulphate - polyacrylamide gel electrophoresis
SEM	scanning electron microscope
siRNA	small interfering RNA
STAT	signal transducers and activators of signaling
TEM	transmission electron microscope
U	unit
ug	microgram
uL	microliter
uM	micromolar
USF	University of South Florida
UV	ultraviolet
VEGF	vascular endothelial growth factor
XTT	2,3-bis-(2-methoxy-4-nitro-5-sulfophenyl)-2H-tetrazolium-5-carboxanilide, disodium salt

Characterization of Novel Nitroplatinum (IV) Complexes for the Treatment of Cancer

Jeannette Lo

ABSTRACT

Many types of chemotherapeutic agents have been developed to target specific mechanisms within the body that control the progression of cancer, though few have been able to circumvent the existing problems associated with the treatments. The current remedies entail grueling drug regimens and toxic side effects that may undermine the effectiveness of the drugs. Cisplatin, a common nitroplatinum(II) drug widely used to treat a variety of cancers, is administered intravenously and circulates systemically, affecting healthy regions of the body as well. Resistance to cisplatin is increasing and the need for new, less toxic medication must be met for future success in cancer therapy. Our lab has synthesized novel nitroplatinum(IV) cisplatin complexes (PH1-14) that may evade these problems. We examined the effects of these compounds on cell viability, as well as effects on cancer-specific mechanisms such as nitric oxide (NO) production, angiogenesis, and the STAT signaling pathways. *In vitro* studies demonstrated that PH1-11 and PH14 demonstrated greater efficacy at inhibiting cell proliferation with lower IC50 values that ranged from 41-58 uM (as compared with cisplatin IC_{50} = 66 uM). Data from NO assays were inconclusive, though there was elevated expression of inducible nitric oxide synthase in cells treated with PH3 and PH11. We also found that PH9 was able to inhibit STAT dimerization at concentrations as low as 0.3 uM. PH9 also decreased VEGF and HIF-1α expression, thereby inhibiting angiogenesis. The activity of

the PH complexes was also studied in C57BL/6 mice inoculated with murine bladder MB49 tumors. The experimental group showed significantly slower tumorigenesis and smaller tumors as compared with the control group. Toxicological analyses of the blood via metabolic assays showed that no nephrotoxicity was observed in dosages of less than 7 mg drug/kg. We conclude from these results the potential for the use of novel mechanisms in the treatment of cancers. This work will guide future investigations of these drugs in further preclinical trials and also introduce an alternative to the traditional chemotherapeutic agents.

CHAPTER 1: BACKGROUND AND SIGNIFICANCE

1.1 Chemotherapy

Chemotherapy is the use of chemotherapeutic agents for the cure, control, and palliation of cancer. Its use has been documented since the 16th century, when heavy metals were used systemically to treat cancers, often causing severe toxicity with limited clinical improvement. Today, chemotherapy is one of the most commonly used treatments for cancer. A wide range of chemotherapeutic drugs have been discovered and are available as treatment, including plant alkaloids, alkylating agents, hormones, and antibiotics. [1]. Continuous research has allowed new drugs to emerge frequently, undergoing clinical trials before being accessible to the public.

Many types of chemotherapeutic agents have been developed to target specific mechanisms within the body that control the progression of cancer. Cell-cycle specific agents, such as Paclitaxel, can arrest metaphase by interfering with the formation of the mitotic spindle. Antimetabolites, such as Floxuidane, are another group of cell-cycle specific agents that act by replacing components essential to the metabolic synthesis of DNA during the S phase. Alkylating agents, such as cisplatin, interrupt replication of genetic material by cross-linking and strand-breaking DNA, leading to cell lysis. Antitumor antibiotics, such as Doxirubicin, prevent cell division by damaging the cell and interfering with DNA and RNA syntheses. Hormones or hormone-like agents,

such as estradiol, inhibit tumor growth by antagonizing the otherwise naturally occurring ligands from their receptors and initiating tumor proliferation [1].

1.2 Platinum Complexes

Cisplatin, a widely used chemotherapeutic agent for the treatment of testicular, ovarian, head and neck, stomach, and bladder carcinomas, is a platinum(II) complex that was discovered in 1972 [2]. Cisplatin can bind to RNA, proteins, and other sulfur-containing biomolecules, though its main biological target is DNA [3-5]. It forms 1,2-intrastrand guanine-guanine, and guanine-adenine crosslinks, accounting for approximately 90% of the resulting adduct. The remaining interactions involve 1,3-intrastrand and interstrand adducts. Its primary crosslink structures serve as a recognition motif for an array of biological molecules, including DNA repair elements, histones, and serum proteins [4, 6]. The formation of these adducts result in blocked transcription, replication inhibition, and apoptosis [3]. However, there are major limitations to cisplatin in anticancer therapy [7].

As a platinum(II) complex, cisplatin circulates systemically in a chemically active state, causing significant side effects including nausea and vomiting, renal toxicity, and bone marrow damage [2, 4, 7-9]. Another limitation to cisplatin is the emergence of resistance to cisplatin during treatment. Studies have reported several modes of resistance such as reduced drug uptake, increased drug inactivation [10, 11], altered drug targets, altered gene expression [12-14], and loss of the DNA mismatch repair (MMR) mechanism [15]. The MMR system plays a critical role in ensuring genomic stability by correcting damaged DNA. MMR is mediated by directing a nick

Figure 1.1 Example structures of platinum(II) and platinum(IV) complexes.

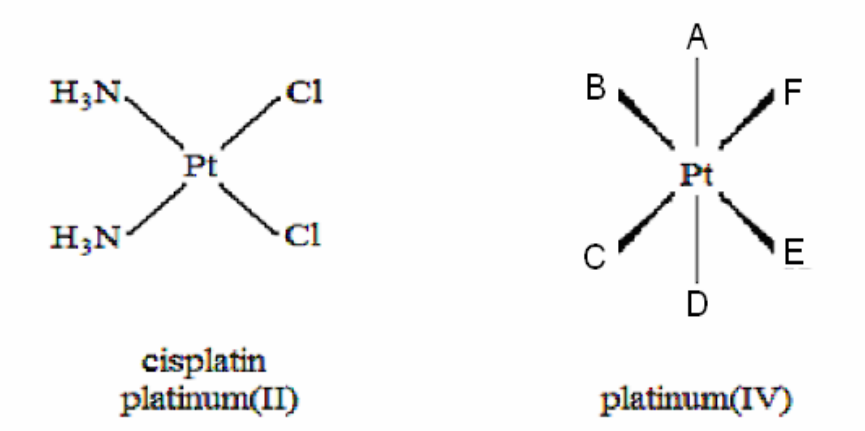

located 5' or 3' to the mismatch. Exonucleated degradation is initiated from the nick to the mismatched base. The DNA that contains the mismatch is then removed, resynthesized, and sealed. In normal cells, MMR recognizes DNA damage and initiates DNA repair or apoptosis. In resistance cells, the MMR system is lost. This decrease in signaling for repair or apoptosis results in increased survival for drug-treated cells [15]. The loss of DNA MMR resulting in cisplatin-resistant cell lines has been documented [16-18].

Improved, platinum-based treatments have emerged. Carboplatin, another platinum(II) drug, was developed to decrease systemic toxicity and resistance observed with cisplatin. However, as compared to cisplatin, carboplatin has inferior efficacy in treating head and neck, bladder, and oesophageal cancers [19]. An alternative to the existing toxic platinum(II) complexes was needed, leading to the development of platinum(IV) complexes. The octahedral platinum(IV) complex are more inert to serum blood proteins as they travels through the body. Then, upon reaching the tumor site,

reduction to a square-planar platinum(II) complex allows the complex to bind to DNA [6]. Ideally, a drug maintaining these properties can be a potent anti-tumor agent with reduced toxic side effects. Additionally, some studies have shown that platinum(IV) complexes can bind to DNA without prior reduction [20, 21].

JM216 (Satraplatin), a platinum(IV) complex, entered clinical trials in 1992 on the basis of possessing several promising preclinical features. It demonstrated potent in vitro and in vivo growth inhibitory properties against several tumor varieties, and has relatively mild toxicity profile with myelosuppression being dose-limiting [22]. Satraplatin is now undergoing investigation in Phase III clinical trails. Zak et al [7] tested another platinum(IV) drug, LA-12, against cisplatin resistant tumor lines and found that LA-12 demonstrated lower IC50's as compared with cisplatin, but had not yet established

Figure 1.2 Platinum complexes designed for the treatment of cancer [2, 7, 9].

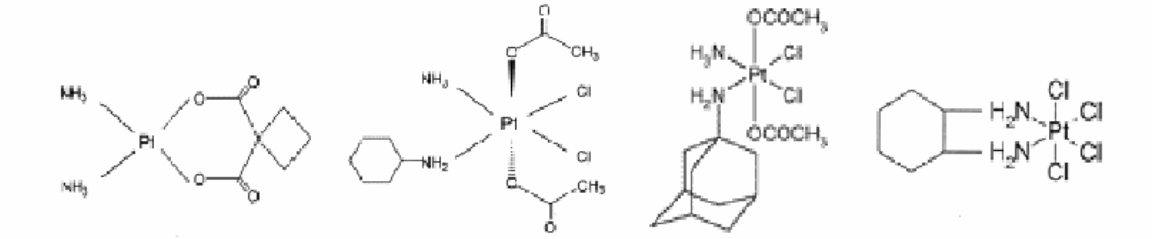

studies for toxicity yet. Tetraplatin, another platinum(IV) analogue, entered Phase I clinical trials to assess toxicities and to determine a maximum tolerated dose. Nausea, vomiting, and myelosuppression were moderate, but neurotoxicity was symptomatic inall patients and caused significant functional impairment some patients, thus ending further

clinical trials [23]. Investigations of additional platinum(IV) complexes are currently in progress.

1.3 Targets and Mechanisms of Cancer Management

1.3.1 Angiogenesis

A cell must have fundamental methods of obtaining nourishment from the body to maintain its health and vitality. Blood vessels facilitate this by carrying oxygen and nutrients to a cell, while removing waste products. Angiogenesis, or the formation of new blood vessels, is usually unique to new or developing tissues. In a healthy adult, emergence of vessels may occur for repair or reproduction but has a limited role. However, in cancer, angiogenesis is integral to its growth. A tumor acquires its own blood supply to sustain its development.

Vascular endothelial growth factor (VEGF) is a pro-angiogenic factor that has been implicated in tumor angiogenesis [24]. Hypoxic inducible factor-1 (HIF-1) is also known to mediate transcription of the gene for VEGF [25]. HIF-1 also plays a role in tumor angiogenesis by mediating P13K/AKT-induced VEGF expression [26-28], pathways that are often found to aberrant in cancers. HIF-1 is a heterodimer comprised of the oxygen-regulated inducible subunit HIF-1α, and a constitutively active HIF-1β [28]. Overexpression of HIF-1α is associated with tumor angiogenesis and tumor cell proliferation and invasion. Drugs that promote inhibition of VEGF have been studied as potential anti-cancer agents [29-31]. Bevacizumab, a recombinant humanized monoclonal antibody directed to VEGF, has been shown in clinical studies to inhibit tumor neovascularization, and thus tumor growth [24]. This suggests that development

of further chemotherapeutic agents targeting VEGF and its related regulators may be useful in cancer therapy.

1.3.2 Signal Transducers and Activators of Transcription (STAT)

Growth factors are secreted extracellularly and bind to receptors on cell membranes to initiate messages to grow or differentiate. Once the growth factor binds, it sets off a cascade of intracellular signaling that may dictate the production of specific protein or gene products, eventually leading to transcription. In cancer, a disruption of this communication system can lead to errors in the under/overproduction of protein products, causing aberrant signaling. Key signaling pathways have been implicated in many cancers.

Signal transducers and activators of transcription (STAT) proteins are a family of cytoplasmic transcription factors that function as downstream effectors of cytokine and growth factor receptor signaling. These proteins transmit signals to the nucleus where STATs bind to DNA and induce gene expression [32-36]. Seven STAT family members have been identified: STAT1, STAT2, STAT3, STAT4, STAT5a, STAT5b, and STAT6 [37]. Numerous studies have shown that constitutively activated STAT1, STAT3, and STAT5 are present in many human cancers [38]. Futhermore, aberrant STAT3 signaling contributes to tumor development through mechanisms of increased cell proliferation. STAT activation occurs when tyrosine kinase activities phosphorylate receptor-bound STATs. The phosphorylated STAT proteins undergo dimerization and translocate to the nucleus, where they bind to specific DNA promoter sequences and induce gene expression [38]. Constitutively active STAT proteins

continue this cascade, resulting in uncontrolled cell proliferation. The use of a chemotherapeutic agent to inhibit STAT dimerization can potentially be a useful technique to treat cancer.

Figure 1.3 Schematic of STAT signaling [39].

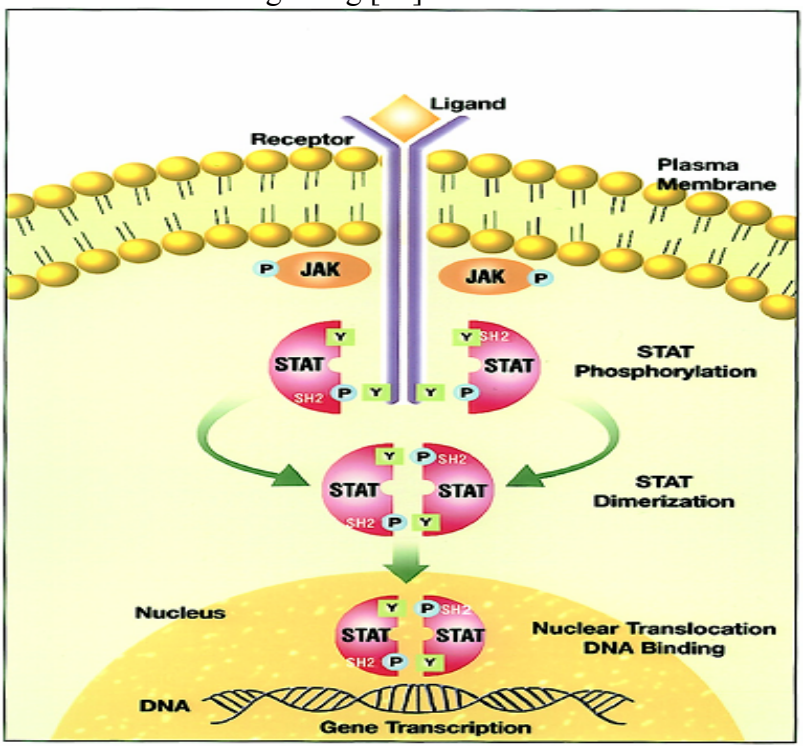

1.3.3 Biological Effects of Nitric Oxide

Nitric oxide (NO) plays a biological role in many pathologies, including diabetes, hypertension, and male impotence. Increasing evidence suggests that NO may also have an effect on cancer biology [40]. Activation of nitric oxide synthase (NOS) and its subsequent release of NO can cause cytostasis [41-43]. It has also been reported that NOS represents a significant macrophage antitumor mechanism [44]. Peroxynitrite, a reaction product of NO with O_2^-, can damage cells [45] and induce apoptosis in a

concentration-dependent manner [46, 47]. Xie and Fidler [48] found that tumor cells that were capable of producing very high levels of NO died *in vivo*, while those cells that produced or were subjected to low levels of NO lived on to undergo clonal selection.

There are several mechanisms for the action of NO, some of which are mediated through the inhibition of DNA synthesis and mitochondrial respiration [49]. This is achieved via interaction with intracellular iron-sulfur prosthetic groups of Complex I and II of the mitochondrial electron transport system together with the citric acid enzyme aconitase, and non-heme iron of ribonucleotide reductase [50-52].

Conflicting data indicate that macrophage infiltration into malignant tissue has been correlated with both a decrease in metastasis and an increase in cell survival [43, 53, 54] However, recent studies suggest that NO may also assist macrophages in their battle against cancer. Several groups found that NO production was a major cytotoxic effector mechanism of macrophages [55-57]. It allowed macrophages to acquire potent antitumor activities after exposure to cytokines.

Additionally, NO can augment the effects of chemotherapy and radiation. Wink et al [58] found that NO can enhance the effect of cisplatin in Chinese hamster V79 cells by inhibiting the DNA repair mechanism. This data supports results from a study by Azizzadeh [59], who also found improved cytotoxicity in Chinese hamster lung fibroblasts using long-acting NO donors. Effects of NO with other drugs have also been reported. Cook et al [60] found that the anticancer action of melphalan improved with NO, while Adams et al [61] discovered that cytotoxic effects of the antimetabolite fludarabine was more potent in human chronic lymphocytic leukemia cells when used

with a NO-donating drug. Radiation therapy has also been found to be enhanced when used in conjunction with NO, due to improved sensitivity to radiation from the cells [62].

1.3.4 Novel Nitroplatinum(IV) Complexes

Our aim in the development of novel nitroplatinum(IV) complexes was to decrease systemic toxicity and resistance, and increase anti-tumor activities through the addition of two ligands to the current square-planar cisplatin structure. Oxidation produces a platinum(IV) complex that has been reported to be able to evade the mechanisms of multi-drug resistance [63-66] and reduce clinical toxicity [2, 3, 65, 67, 68]. This new group of platinum(IV) compounds can circumvent the drug-resistance commonly observed with traditional anti-cancer agents such as cisplatin. They may prevent the direct extrusion of cytotoxic drugs from the cell, or may act by inhibiting the sequestering of the drugs into intracellular compartments, thereby reducing effective intracellular drug concentrations [69]. The prevention of these self-preserving actions can lead to successful drug administration.

CHAPTER 2: EXPERIMENTAL DESIGN

2.1 *In vitro* studies

2.1.1 Drug Synthesis

In compliance with the regulations of patents and licensing, the details of synthesis of these platinum(IV) complexes under patents #03B100 and #03B005 cannot be disclosed at this time.

2.1.2 Cell Culture

The human lung carcinoma cell line A549 was generously provided by Dr. George Blanck (Dept. of Biochemistry, College of Medicine, USF). Frozen cells were thawed at 23˚C and grown in 45% Dulbecco's Modified Eagle Medium:45% Ham's F12 Medium:10% Newborn Calf Serum (Fisher Scientific). L-glutamine, penicillin-streptomycin, and sodium pyruvate (Fisher Scientific) were added to media for final concentrations at 3 mM, 100 U/mL, and 1 mM, respectively. Media was filter-sterilized using vacuum filtration through a polyethersulfone membrane of 0.2 micron pore size. Cells were grown in canted-neck vented-cap tissue culture flasks (BD Falcon) in a 37˚C incubator (NuAire) with 7.5% CO_2 and seeded at confluence.

2.1.3 Drug treatment

Cells in log phase were seeded at 90-100% confluence. Cells were washed twice with 1x phosphate buffered saline (PBS), then lysed from culture flasks

with trypsin-versene (Cambrex Bio Science). Cells were seeded into 96-well tissue culture plates (growth area per well = 0.32 cm^2) at a density of 2.5 x 10^5 cells per well. Drug and media were added to the wells in varying concentrations for a final total volume of 200 uL per well. Culture plates were then incubated for 48 hours at 37˚C with 7.5% CO_2. Each treatment condition was performed in triplicate. Controls contained only cells and media.

Table 2.1. Schema of drug treatment at various dilutions.

Treatment Condition	Cell volume (uL)	Media (uL)	Drug volume (uL)
Control	100	100	0
10 uM drug	100	90	10
20 uM drug	100	80	20
25 uM drug	100	75	25
30 uM drug	100	70	30
40 uM drug	100	60	40
50 uM drug	100	50	50
60 uM drug	100	40	60
70 uM drug	100	30	70
75 uM drug	100	25	75

2.1.4 XTT Cell Viability Assay

Cell viability was determined using the tetrazolium salt XTT [2,3-bis-(2-methoxy-4-nitro-5-sulfophenyl)-2H-tetrazolium-5- carboxanilide, disodium salt] Cell Proliferation Kit (MD Biosciences, Switzerland). The XTT assay is a biochemical procedure that allows for the assessment of viable cells. Mitochondrial dehydrogenases in metabolically active cells cleave the tetrazolium ring, producing a water-soluble

orange formazan dye. The amount of dye produced is proportional to the number of live cells. This dye can then be measured using a spectrophotometer [67].

After drug treatment as described in section 2.1.3, the XTT reagent was prepared by adding 0.2 ml of the PMS (N-methyl dibenzopyrazine methyl sulfate) activation reagent to 10 ml of the XTT reagent. This produced enough reaction mixture for the analysis of one 96-well plate. One-hundred microliters of the XTT reaction solution was added to each well (final XTT concentration = 0.3 mg/ml). Plates were incubated for an additional 2-5 hours at 37˚C with 7.5% CO_2. The plates were then agitated on a plate shaker for approximately 5 minutes and immediately analyzed for absorbance at 475 nm using a UV-Visible spectrophotometer fitted with a fiber optic probe (Varian, CA). Control wells were run with each trial and contained cells, media, and XTT reagent.

The spectrophotometer generates absorbance values in arbitrary units. Our % survival (relative to controls) values were determined by calculating the average absorbance values of triplicate wells, then dividing that average by the average control absorbance value for that trial. The 50% inhibitory concentration (IC_{50}) values were determined using a linear trendline generated by the Excel program (Microsoft). A scatter plot of the cell viability data was created as a function of drug concentration, then a linear trendline equation for each drug was determined by the software such that the x-axis depicted drug concentration values, and the y-axis depicted % survival (relative to controls). The value of "50" was substituted for the "y" variable in the equation to obtain the IC_{50} value.

2.1.5 MTT Cell Viability Assay

Cell viability was also determined using the tetrazolium salt MTT Cell Proliferation Assay Kit (Molecular Probes). The MTT assay operates under the same principles as the XTT. The assay involves the conversion of the water soluble MTT (3-(4,5-dimethylthaizol-2-yl)-2,5-diphenyltetrazolium bromide) into an insoluble purple formazan dye. The amount of dye produced is proportional to the number of live cells. The aqueous contents are then removed and the dye is then dissolved in DMSO and quantified using a spectrophotometer.

After drug treatment as described in section 2.1.3, 20 uL of the MTT reagent (5 mg/ml) was added to each well. Plates were incubated for an additional 3 hours at 37˚C with 7.5% CO_2. The plates were then agitated on a plate shaker for approximately 5 minutes. The liquid content of the wells were aspirated out and discarded. To dissolve the dye product, 200 uL of DMSO was added to each well. The plates were agitated again until the dye crystals were completely dissolved. Samples were immediately analyzed for absorbance at 570 nm using a UV-visible spectrophotometer (Varian, CA) with fiber optic probe. Control wells were run with each trial containing cells, media, and MTT reagent. Relative survival and IC_{50} values were calculated as described in section 2.1.4.

2.1.6 Nitric Oxide Production

The quantity of nitric oxide produced was determined using the DAF-FM (4-amino-5-methylamino-2',7'- difluorofluorescein) Diacetate Reagent Kit (Molecular Probes, OR). The DAF-FM diacetate assay is based on the reactivity of aromatic vicinal

diamines with nitric oxide (NO) in the presence of oxygen [70]. The non-fluorescent DAF-FM diacetate passively diffuses through the cell membrane and is de-acetylated by intracellular esterases to become DAF-FM. The reaction of the weakly fluorescent DAF-FM with NO transforms DAF-FM to an intensely fluorescent benzotriaole derivative, which can be measured for fluorescence using a fluorimeter [70, 71].

Figure 2.1 Mechanism of DAF-FM assay. Schema adapted from Molecular Probes [72].

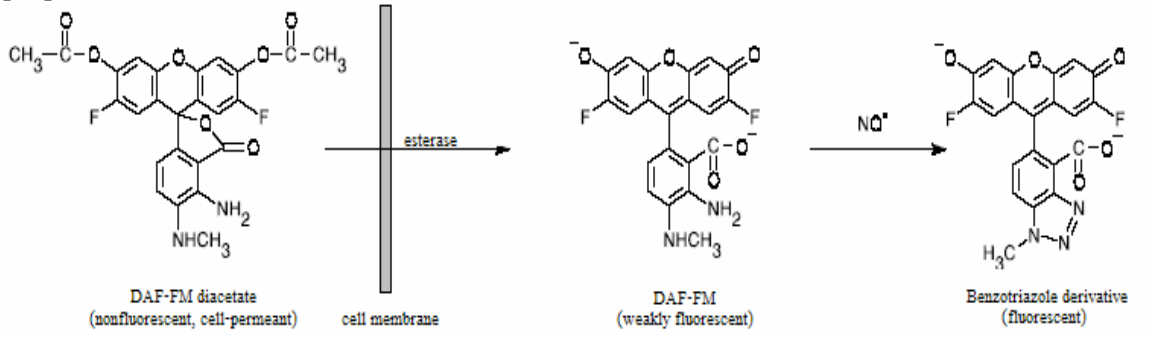

Drug treatment was performed as described in section 2.1.3 using phenol-red free DMEM media (Biowhittaker). The DAF-FM diacetate reagent was prepared by dissolving 50 ug of the reagent powder with 20 uL of molecular biology grade DMSO [dimethylsulfoxide] (Fisher Scientific). The solution was then diluted with media to produce a 105 uM working solution. Ten microliters of the working solution was added to each well. The plates were incubated with the working solution (final DAF-FM diacetate concentration = 5 uM) for 30-120 minutes at 37˚C with 7.5% CO_2. The plates were then agitated on a plate shaker and immediately analyzed for fluorescence via a fluorescence spectrophotometer (Varian, CA). Fluorescence spectrophotometer settings were as follows: excitation wavelength = 495 nm, emission wavelength = 515 nm,

excitation slit = 5 nm, and emission slit = 5 nm. Each treatment condition was performed in triplicate. Control wells containing cells, media, and DAF-FM acetate were run with each trial.

2.1.7 Western Blotting

To determine the expression level of inducible nitric oxide synthase (iNOS) in cells, a Western Blot was performed. Cells were grown and treated at 40 uM as described in sections 2.1.2 and 2.1.3. Cells were harvested by trypsinization and lysed with a hypotonic buffer. Equivalent quantities of protein from each sample were separated by SDS-PAGE on 4-15% Tris-HCl Ready Gels (Bio-Rad). Following electrophoresis, proteins were transferred to Immobilon-P membranes (Millipore) using a wet transfer method (Bio-Rad). Membranes were blocked for 1 h in 5% nonfat dry milk in Tris-buffered saline-Tween-20 and subsequently washed. Membranes were incubated with polyclonal iNOS antibody (Santa Cruz, SC-651) in 5% nonfat dry milk for 1 h. Following washing, membranes were incubated with a secondary antibody in 5% nonfat dry milk for 1 h. The signal was visualized by chemiluminescence using ECL reagent (Amersham Biosciences) and then exposed to film. Band intensities were quantitated using ImageQuant software (Molecular Dynamics) [73]. This blot was graciously run by Laura Pendleton (Dept. of Biochemistry, USF).

To determine the levels of HIF-1α and VEGF expression, DU145 prostate cancer cells were serum-starved for 20 h in serum-free media and treated with PH9 for 6 hours. Fifty μg of nuclear or whole-cell extracts was used. HIF-1α rabbit polyclonal antibody (H-206) (1:500 dilution) and anti-VEGF monoclonal antibody (1:1,000 dilution)

were used for the Western blot. Horseradish peroxidase-conjugated sheep anti-mouse and donkey anti-rabbit or anti-goat secondary antibodies were used at 1:2,000 and 1:5,000 dilutions, respectively. The signal was developed with SuperSignal West Pico Chemiluminescent Substrate (PIERCE). These blots were kindly run by the Yu lab (Dept. of Interdisplinary Oncology, Moffitt Cancer Center).

2.1.8 Energy-dispersive X-Ray Analysis of Platinum-Treated Cells

Localization of the intracellular platinum-based drugs was attempted with electron microscopy. Cells were grown to confluence (~2-6 x 10^6 cells) as described in section 2.1.2 in a sterile 10 cm^2 glass Petri dish. Cells were incubated with 55 uM of drug for 48 hours. The cells were then washed twice with 1x PBS and fixed overnight with 2.5% glutaraldehyde in 0.1 M phosphate buffer at room temperature. The fixative was aspirated and saved. The cells were rinsed with PBS, then dehydrated in a graded series of ethanol as follows: 35% ethanol, 70% ethanol and 95% ethanol, 5 minutes each at room temperature. Cells were then scraped from the Petri dish and infiltrated with a 50:50 mix of 95% ethanol:L R White acrylic resin in a microcentrifuge tube for 1 hour at room temperature. The cells were infiltrated in two 1-hour changes of 100% L R White at room temperature, then infiltrated overnight in L R White at 4˚C. The following day, cells were incubated twice in fresh changes of L R W Localization of the intracellular platinum-based drugs was attempted with electron microscopy. Cells were grown to confluence (~2-6 x 10^6 cells) as described in section 2.1.2 in a sterile 10 cm^2 glass Petri dish. Cells were incubated with 55 uM of drug for 48 hours. The cells were then

washed twice with 1x PBS and fixed overnight with 2.5% glutaraldehyde in 0.1M phosphate buffer at room temperature. The fixative was aspirated and saved. The cells were rinsed with PBS, then dehydrated in a graded series of ethanol as follows: 35% ethanol, 70% ethanol and 95% ethanol, 5 minutes each at room temperature. hite at room temperature. Following the last resin change, cells were placed in a gelatin capsule, which was then filled with the resin. The resin was polymerized at 50˚C overnight (~15 hours).

Following polymerization, the block of cells was sectioned on a Reichert Ultracut ultramicrotome using a diamond knife. Sections at 0.25 microns and 90 nm, were obtained. The sections were picked up on 200 mesh nickel grids and examined without further staining with a Philips CM10 transmission electron microscope equipped with an EDAX 9900 energy-dispersive x-ray analyzer. The microscope was operated at 60 kV. A spot size of 100 nm was used to examine the cells. X-ray spectra from the nuclei, cytoplasm and cell membrane were collected at a count rate of 250 cps. A platinum aperture for the microscope was inserted into the beam to serve as a positive-platinum control.

Additional cells were desiccated from either ethanol or distilled water onto carbon sample holders and examined as bulk samples by scanning electron microscope (SEM) with EDAX analysis. Dried cells were examined with and without a carbon coating at 30 kV in a Philips 515 SEM with the EDAX analyzer. A spot size of 100 nm was also used to collect x-ray data in the SEM. The cell nuclei and cytoplasm were examined in this study. A drop of the fixative was also air-dried on a sample holder and

examined by SEM-EDS to detect for possible levels of platinum that may have diffused out of the cells.

The EDAX analyzer is able to detect concentrations of 0.5% for heavy elements such as platinum. Under ideal conditions, the analyzer may detect levels as low as 0.25% concentration of an element in a sample.

2.1.9 Electrophoretic Mobility Shift Assay (EMSA)

Cells were grown and treated with drugs as described in section 2.1.2 and 2.1.3. Nuclear extracts from the cells were used for electrophoretic mobility gel shift assays (EMSA) as described by Turkson et al. [74]. Briefly, nuclear extracts containing STAT3 and STAT1 were prepared from human lung non-small cell line A549, and pre-incubated with various concentrations of PH compounds for 30 minutes. Volumes containing equal amounts of total protein were then incubated with ^{32}P-labeled hSIE oligonucleotide probe, which expresses high affinity sis-inducible elements that selectively bind STAT1 or STAT3. The resulting DNA-protein complexes were analyzed by EMSA for the STAT-related DNA-binding factors. This work was performed by the Jove lab (Dept. of Interdisciplinary Oncology, Moffitt Cancer Center).

2.2 *In vivo* studies

2.2.1 Animal Housing and Treatment

Male, 8-week-old athymic mice used in these experiments were obtained from Jackson Laboratories and were cared for in accordance with the guidelines of IACUC under protocol #R2426 . Animals were caged in groups of four and housed in

conventional condition in a temperature-controlled vivarium (23°C) on a reverse light/dark cycle. Food and water were available *ad libitum.* The mice were acclimated to the housing environment for 7 days prior to testing. At week 2 of the study, mice received subcutaneous injections of A549 cells in PBS (1 x 10^7 cells/ flank) into the right flank. Tumors grew to a palpable size by week 3.

Mice were randomly distributed into four groups of 12 mice. Three treatment and one control group were defined as: (1) Group 1: drug treatment with 7 mg PH9/kg body weight, (2) Group 2: drug treatment with 7 mg PH14/kg body weight, (3) Group 3: drug treatment with 7 mg PH12/kg body weight, and (4) Group 4: control treatment with saline. The treatment groups received a series of three 0.2 mL injections of the drug dissolved in DMSO (20%) with saline vehicle (80%) into the tail vein. The control group received only saline:DMSO vehicle. Blood from the saphenous vein was collected from the animals weekly into heparin-gel tubes. Urine was collected during routine weighings. All procedures were performed during the dark phase of the light-dark cycle. Animals were euthanized at the 8th week of the study and the organs were harvested and frozen for future work.

One compound, PH9, was selected for further *in vivo* toxicity testing. Yu et al carried out mouse studies as previously described [75]. Briefly, 7 to 8 week-old C57BL/6 male mice (NCI, Frederick, MD) were maintained under pathogen-free conditions in accordance with established institutional guidance and approved protocols. The animals received subcutaneous injections of murine bladder tumor MB49 cells (5 x 10^5 cells/ flank) into the right flank. The tumors were allowed to grow to 3-5 mm in diameter. Tumor sizes were recorded weekly with Vernier calipers. Over the course of

two weeks, four tail vein injections of PH9 (5 mg/kg) were administered to the treatment group. The control group received only vehicle (10% DMSO/PBS). Animals were euthanized within 1-3 days of the last injection using a CO_2 chamber. Blood was immediately collected via cardiac puncture using a 1 cc syringe, and transferred in heparin-gel tubes.

2.2.2 Toxicology

Analyses of toxicity were determined by quantifying levels of enzymes and proteins present in blood and urine. The detection of glucose and glutamic acid concentrations in the urine was mediated by an Amplex Red Glucose Assay Kit and Amplex Red Glutamic Acid Assay Kit, respectively (Molecular Probes). All procedures were conducted in accordance with the instructions provided by the manufacturer [76, 77]. Briefly, stock and working solutions were prepared by combining 1X reaction buffer, horseradish peroxidase, and assay reagent. A standard curve was created by diluting glucose in 1X reaction buffer. Each urine sample was diluted in 1X reaction buffer. Fifty microliters of the working solution was added to microplate wells containing 50 uL of sample or control specimen. The plates were incubated at either room T in ambient air or at 37˚C with 7.5% CO_2 depending on kit instructions. Plates were agitated briefly on a plate shaker and then immediately measured for fluorescence using a fluorescence spectrophotometer. Fluorescence spectrophotometer settings were as follows: excitation wavelength = 530 nm, emission wavelength = 590 nm, excitation slit = 5 nm, and emission slit = 5 nm. Background fluorescence was accounted for by

subtracting control absorbance values from sample values. Glucose/glutamic acid values were determined from the absorbance readings by comparison to the standard curve.

The detection of albumin, alanine aminotransferase (ALT), and blood urea nitrogen (BUN) concentrations from serum samples was mediated by Amplex Albumin Reagent, ALT Reagent, and BUN Reagent assay kits, respectively (Amresco). All procedures were conducted in accordance with the instructions provided by the manufacturer[78-80]. Briefly, blood samples were collected in heparin-gel blood collection microtubes. The tubes were centrifuged at 2,000 xg for 10 minutes. Serum was separated from the clot immediately and kept on ice or at 4˚C until analysis. Assays were performed within 24 hours of blood collection. Working solutions were prepared by reconstituting stock reagent powder with 50 uL deionized water. Working solution was incubated for the designated time in a 37˚C water bath. Samples and controls were added to the solution and incubated again. The absorbencies were measured by a UV-visible spectrophotometer with fiber optic probe at wavelengths unique to each assay kit.

Toxicological analysis of the 17 blood samples collected from C57BL/6 mice was performed using the Vitros 950 automated chemical analyzer (Ortho Clinical Diagnostics).

2.2.3 Angiogenesis

To assess for the effect of PH9 on angiogenesis, athymic mice (NCI) were maintained by Yu et al as described in section 2.2.5. Matrigel assays were performed as described previously [81]. Briefly, 2 x 10^6 MCF-7 tumor cells stably transfected with either an empty control vector or Stat3siRNA expression vector were suspended in 100 μl

PBS and mixed with 0.5 ml of Matrigel (Collaborative Biochemical Products) on ice, followed by injection subcutaneously into the abdominal midline of nude nice. Matrigel plugs were harvested for photography and assaying hemoglobin contents. Hemoglobin quantification was carried out by the Drabkin method.

CHAPTER 3: RESULTS AND DISCUSSION

3.1 Cell Viability

Cell viability is a critical factor to consider when determining the effect of a chemotherapeutic agent on cells. The use of XTT in the enumeration of viable cells after drug treatment can indicate if the agent is effective in killing cells, but can also indicate cytotoxicity as well [67, 82]. To identify the optimal experimental conditions, preliminary data was generated from a range of treatment parameters at the beginning of the study. An analysis of 14 novel nitroplatinum (IV) compounds and cisplatin at various treatment concentrations revealed that cell viability was not markedly affected at concentrations below 30 uM for all incubation times measured (data not shown). Cell viability data for these compounds was also collected for a range of incubation times with the XTT reagent. Table 3.1 summarizes the average relative survival values and standard deviations for the drugs at incubations times of 2-5 hours at drug treatment concentration of 50 uM. Absorbance data of treated cells is presented as % survival (treated absorbance / control absorbance). It was determined that incubation of the cells with the XTT reagent between 3-5 hours yielded reliable data with the low standard deviations between triplicate wells of the same treatment. This data lie within the range of the suggested incubation times as recommended by the reagent manufacturer. These drug concentrations and reagent incubation times were used in subsequent experimentations.

Table 3.1 Relative survival for A549 cells treated with 50 uM PH compounds as a function of XTT incubation time.

Drug	2h	3h	4h	5h
Cisplatin	62.0 +/- 4.1	63.4 +/- 1.6	62.2 +/- 0.4	72.1 +/- 0.7
PH1	57.5 +/- 1.3	57.6 +/- 1.0	56.7 +/- 1.0	61.6 +/- 1.4
PH2	77.7 +/- 4.1	73.6 +/- 2.5	73.4 +/- 1.1	80.0 +/- 1.4
PH3	53.6 +/- 2.3	53.4 +/- 0.6	52.0 +/- 0.7	56.2+/- 1.0
PH4	57.3 +/- 0.7	57.3 +/- 0.5	55.6 +/- 0.6	60.7 +/- 0.9
PH5	54.0 +/- 2.5	54.8 +/- 0.6	53.5 +/- 0.7	58.4 +/- 1.1
PH6	55.8 +/- 0.5	55.6 +/- 0.3	54.3 +/- 0.5	59.2 +/- 0.8
PH7	57.5 +/- 1.6	57.7 +/- 0.3	56.8 +/- 0.7	62.9 +/- 0.7
PH8	54.7+/- 1.4	54.7 +/- 1.1	54.2 +/- 0.7	58.8 +/- 1.2
PH9	54.9 +/- 0.7	55.6 +/- 0.9	54.2 +/- 0.9	58.6 +/- 1.0
PH10	54.0 +/- 0.5	53.6 +/- 0.3	52.7 +/- 0.9	56.5 +/- 0.8
PH11	56.1 +/- 0.1	55.6 +/- 0.0	55.2 +/- 0.1	59.3 +/- 0.2

Figure 3.1 Relative survival for cells were treated with PH1-4 and cisplatin.

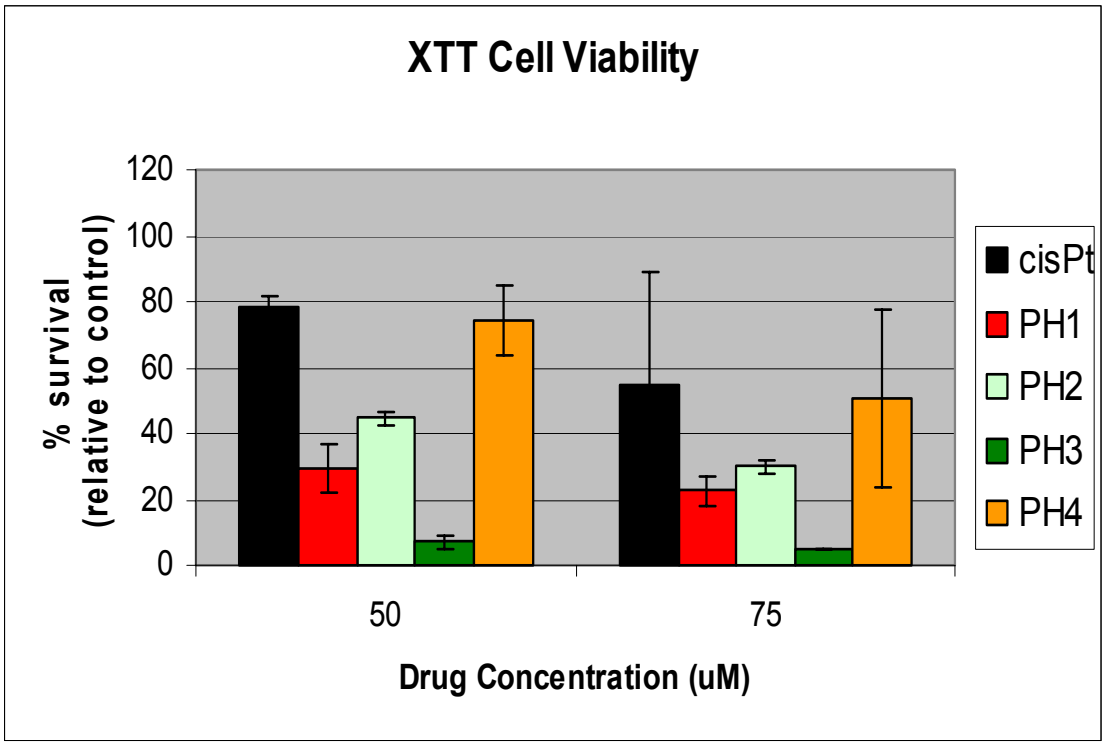

Twelve of the fourteen compounds were better cell proliferation inhibitors than cisplatin when compared at the same concentration. This observation is in agreement with other studies of platinum(IV) compounds [2, 83, 84]. As demonstrated in Figure 3.1, all cells treated with PH1-PH4 at concentrations of 50 uM and 75 uM had lower survival percentages than cisplatin. Their calculated IC_{50} were also lower than that of cisplatin. Table 3.2 shows the IC_{50} values for these drugs. This data suggests that lower dosages of the PH compounds can be used to inhibit tumor cell growth when compared to dosages of cisplatin. It is evident that the calculated IC_{50} value for PH4 is unlikely to be a valid value. This error may be due to incorrect drug dosing or improper cell distribution during experimentation. Analyses for PH4 were repeated in later experiments.

Table 3.2 Calculated IC_{50} values for PH1-4 and cisplatin from XTT Assay.

Drug	Calculated IC_{50} (uM)
Cisplatin	80
PH1	31
PH2	41
PH3	-405
PH4	76

Subsequent trials run with these and other PH compounds resulted in similar inhibition effects as compared to cisplatin. Figures 3.2 and 3.3 depict the percent survival percentages for compounds PH4-11. Again, the novel compounds performed significantly better than cisplatin. At concentrations of 60 uM or greater, there is almost no survival of cells. Table 3.3 summarizes the IC_{50} values for these drugs. Cisplatin has an IC_{50} of 71 uM, while the PH compounds inhibited 50% of the cell growth at concentrations near 45 uM. The IC_{50} values for the PH compounds are consistently lower than that of cisplatin.

Figure 3.2 Relative survival for cells were treated with PH4-8 and cisplatin.

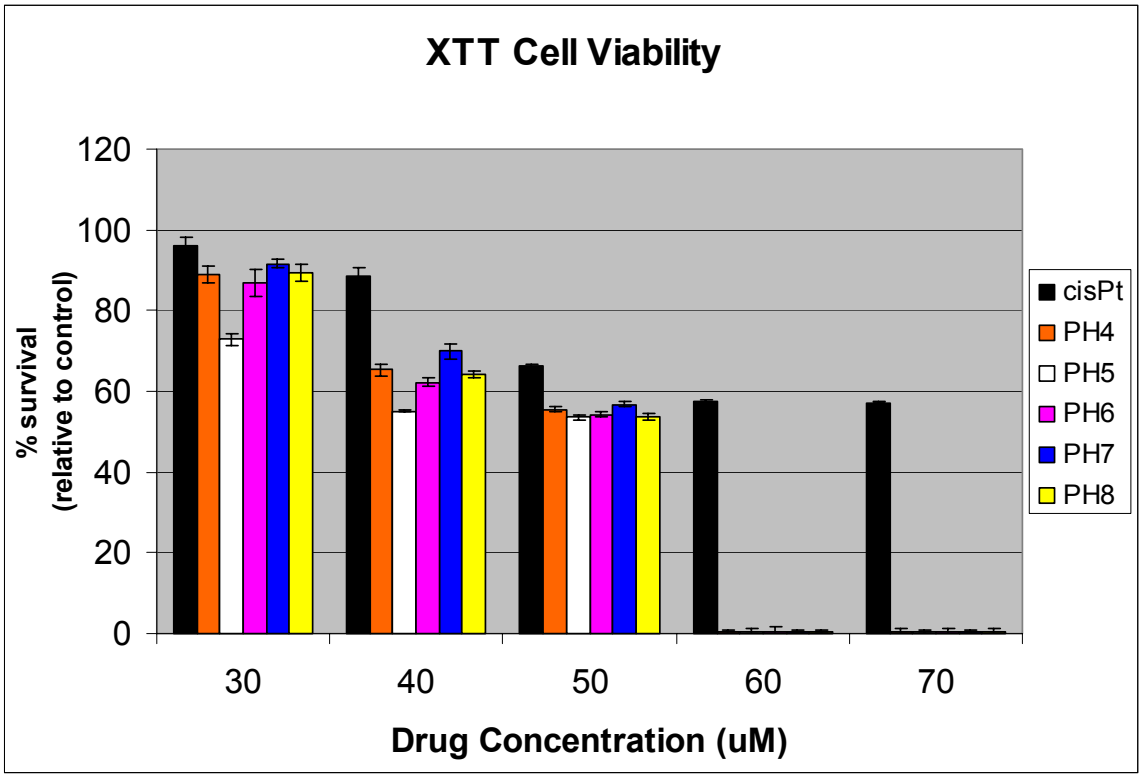

Figure 3.3 Relative survival for cells were treated with PH1-3, 9-11 and cisplatin.

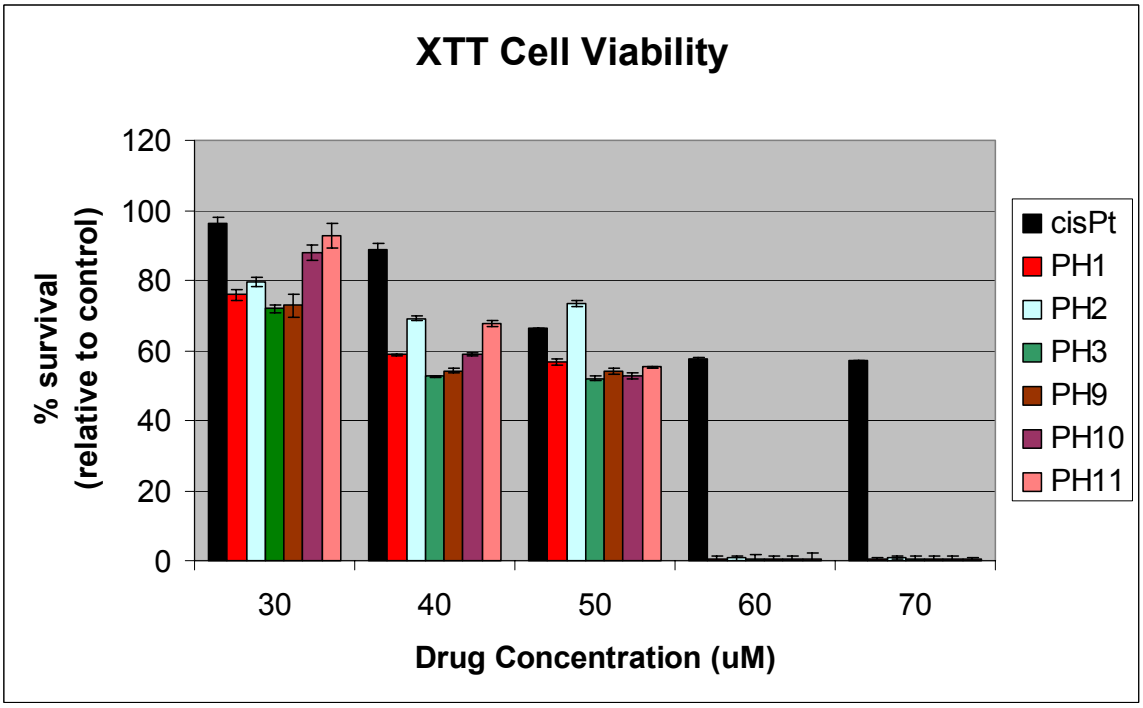

Table 3.3 Calculated IC_{50} values for PH1-11 and cisplatin from XTT Assay.

Drug	Calculated IC_{50} (uM)
Cisplatin	71
PH1	44
PH2	48
PH3	43
PH4	47
PH5	43
PH6	46
PH7	48
PH8	47
PH9	43
PH10	46
PH11	47

Figure 3.4 depicts the relative survival percentages for four of the previously tested compounds and three other compounds PH12-14. This experiment gathered conflicting data as compared to the previous studies. The activity of cisplatin appeared to be better than that of both the previously characterized novel compounds and the untested compounds. IC_{50} values for the nitroplatinum (IV) compounds were also significantly higher than values previously shown, though cisplatin actually demonstrated a lower IC_{50} value. Table 3.4 shows these results.

The ligands of compounds PH12 and PH14 are structures which may potentially have a proliferative affect on cells, in agreement with the results. However, in this set of data, better proliferation is observed for the other PH compounds that had previously been found to be efficient inhibitors of tumor cell growth. This observation, suggests that the discordant data from this trial may is questionable. Possible sources of error include equipment malfunction, technical mistakes, and unfavorable environmental conditions for study. It can also be considered that the data from Figure 3.1 – 3.3 may

Figure 3.4 Relative survival for cells were treated with PH3,4,9-14 and cisplatin.

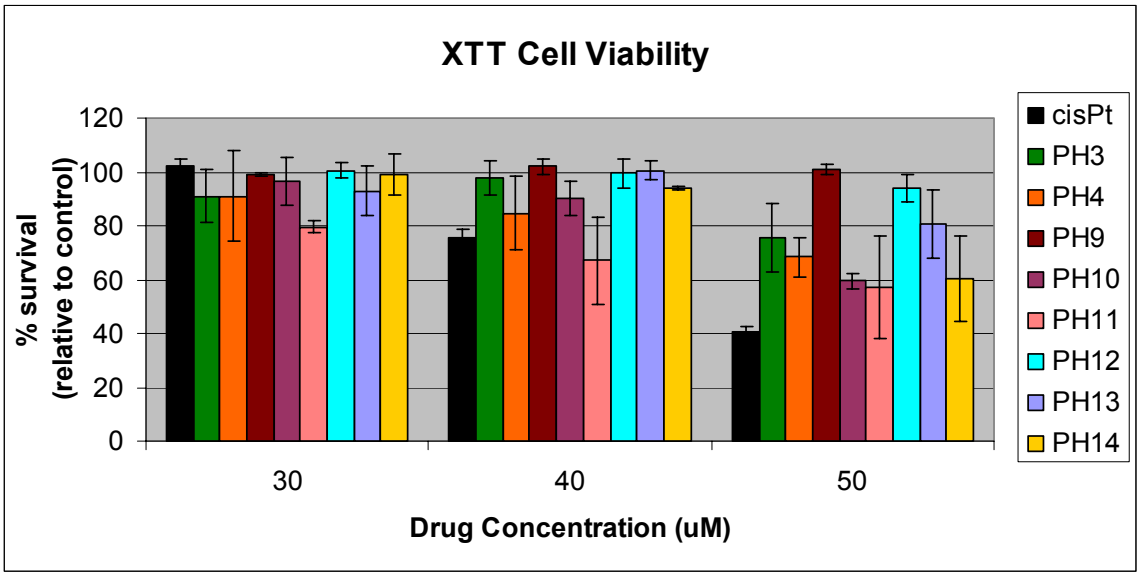

Table 3.4 Calculated IC_{50} values for PH3,4,9-14 and cisplatin from XTT Assay.

Drug	Calculated IC_{50} (uM)
Cisplatin	47
PH3	90
PH4	68
PH9	545
PH10	57
PH11	56
PH12	191
PH13	107
PH14	58

not be reliable, and further studies need to be conducted to produce repeatable, reliable results for all compounds.

Assays of cell viability performed with MTT showed similar results to the earlier XTT assays. Table 3.5 summarizes representative data from the MTT assays. The calculated IC_{50} values for most compounds closely resemble those from the XTT

Table 3.5 Calculated IC_{50} values for PH1,3,4,7-11 and cisplatin using the MTT assay.

Drug	Calculated IC_{50} (uM)
Cisplatin	63
PH1	50
PH3	41
PH4	56
PH7	61
PH8	506
PH9	45
PH10	54
PH11	53

assay, suggesting that there is agreement between the two assay types and thus that the data is reliable. This agreement can implicate key drugs that should be further explored.

A summary of the IC_{50} values for the XTT and MTT assays are shown in Table 3.6. Despite the conflicting results from XTT3 (data from third XTT trial), the overall data suggests that some of these PH compounds may have the potential to serve

Table 3.6 Summary of calculated IC_{50} values from XTT and MTT assays.

	XTT1	XTT2	XTT3	MTT	Avg +/- SD
Cisplatin	80	71	47	63	65.3 +/- 12.1
PH1	31	44		50	41.7 +/- 7.9
PH2	41	48			44.5 +/- 3.5
PH3	-	43	90	41	58.0 +/- 22.6
PH4	76	47	68	56	61.8 +/- 11.1
PH5		43			43
PH6		46			46
PH7		48		61	54.5 +/- 6.5
PH8		47		506	276.5 +/- 229.5
PH9		43	545	45	211 +/- 236.2
PH10		46	57	54	52.3 +/- 4.6
PH11		47	56	53	52.0 +/- 3.7
PH12			191		191
PH13			107		107
PH14			58		58

as potent anti-tumor agents at low doses. The enhanced activity of the PH compounds as compared to cisplatin may be due to the action of the additional ligands on the novel compounds which are not present in cisplatin. The additional activities of these compounds are investigated in subsequent sections.

3.2 Nitric Oxide Production

As the platinum(IV) compounds reduce to a platinum(II) state in the cell, the release of its axial nitro-ligands is expected [6]. These ligands eventually form nitric oxide, which has been shown to have potent anti-tumor activities [40]. An assessment for the presence of NO was mediated by the DAF-FM diacetate assay. Initial trials of this assay were performed with media containing phenol-red. It was later discovered that phenol-red media may interfere with fluorescence readings[72]. These data sets were discarded. Unexpected problems also arose with the alignment of the plate reader of the fluorimeter during this study. Efforts were made to rectify the fluorescence interference by replacing the standard media with phenol-red free media during the drug treatment phase of the experiment. The plate reader was re-aligned and tested for operation using fluorescein (excitation wavelength = 492 nm, emission wavelength = 519 nm, excitation slit = 5 nm, and emission slit = 5 nm).

Results from the DAF-FM diacetate assays are inconclusive. Figure 3.5A shows the results of a DAF-FM diacetate assay after incubation with the reagent for 120 minutes. The level of NO production does not appear to have a dose-response relationship until the drug concentration reaches 40 uM. After this point, the amount of NO production correlates with drug dose. This phenomenon may be related to the data

from proliferation assays showing that at drug concentrations of 30 uM and below, cell survival is relatively unaffected. This suggests that the PH compounds had little effect on NO production at concentrations below 40 uM. Thus, if these compounds are causing NO release, the % NO production should be comparable to the control NO production, or near 100%. However, most levels fall below 100%. At higher drug concentrations, the

Figure 3.5A Trial 1 results of NO production.

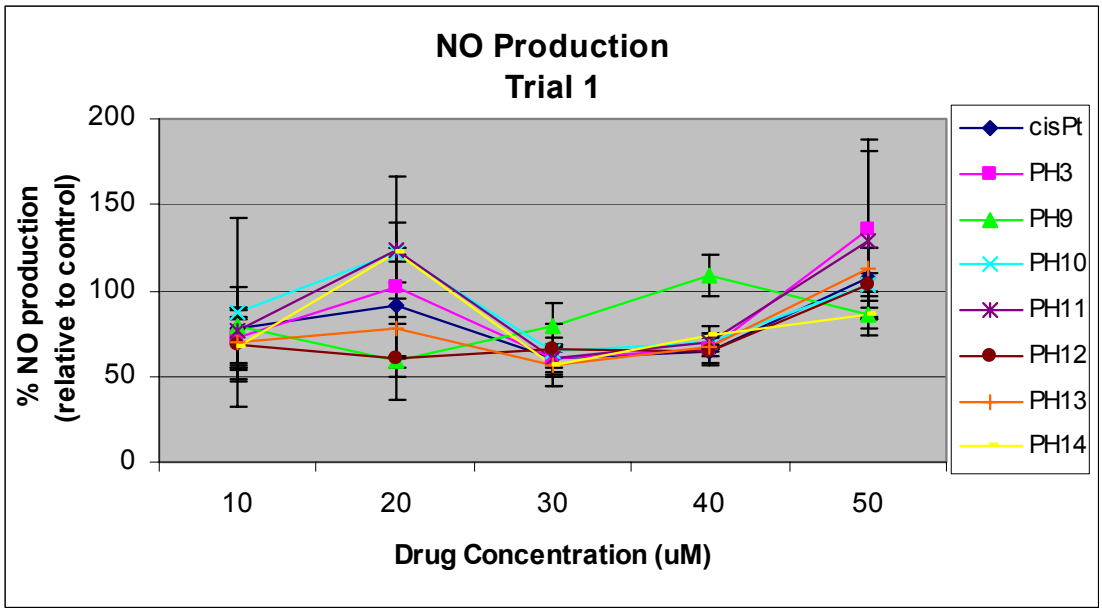

PH compounds will begin to play a role in the production of NO. As drug concentration increases, cell survival drops. Since the data of NO production represents each well and not the rate per cell, it is expected that the relative NO production percentages underestimate true values because there are fewer cells per treated well as compared to control wells. Therefore, the dose-response relationship is expected to be even stronger than shown in Figure 3.5A. Relative to cisplatin, only cells treated with PH3, PH11, and PH13 seem to exhibit greater NO release. It cannot be determined at this time if these

compounds are effective NO producers since their values as compared to controls have not been correlated with cell number.

It is evident that the standard deviations of the data points as depicted by the error bars are large. This variation is believed to be due to the extreme sensitivity of the assay reagent, and the possibility of small variations in the number of cells between wells. This standard deviation was observed in the controls as well. It is important to note that fluorescein, which was included in the fluorimeter readings to control for read error, showed very little deviation between triplicate wells (data not shown). This observation demonstrates that inaccuracy of fluorimeter readings can be eliminated as a source of error.

Figures 3.5B-D show the results of additional DAF-FM assays. The data here does not provide insight into the abilities of these compounds to induce NO release. Figures 3.5B and 3.5C indicate that cells treated with all compounds including cisplatin had higher NO release than untreated control cells. However, results depicted in Figure 3.5D concurs with the data from Figure 3.5A in that the PH compounds were ineffective in eliciting NO release. It is apparent that there is little agreement for % NO production values between the various trials, but there is evidence that cisplatin treated cells generate higher NO values than the PH compounds. This outcome was not expected since some of the PH compounds were designed for this purpose. However, these results do not conclusively indicate that the PH compounds are ineffective generators of NO, but rather that further studies need to be conducted to accurately measure NO production.

Figure 3.5B Trial 2 results of NO production.

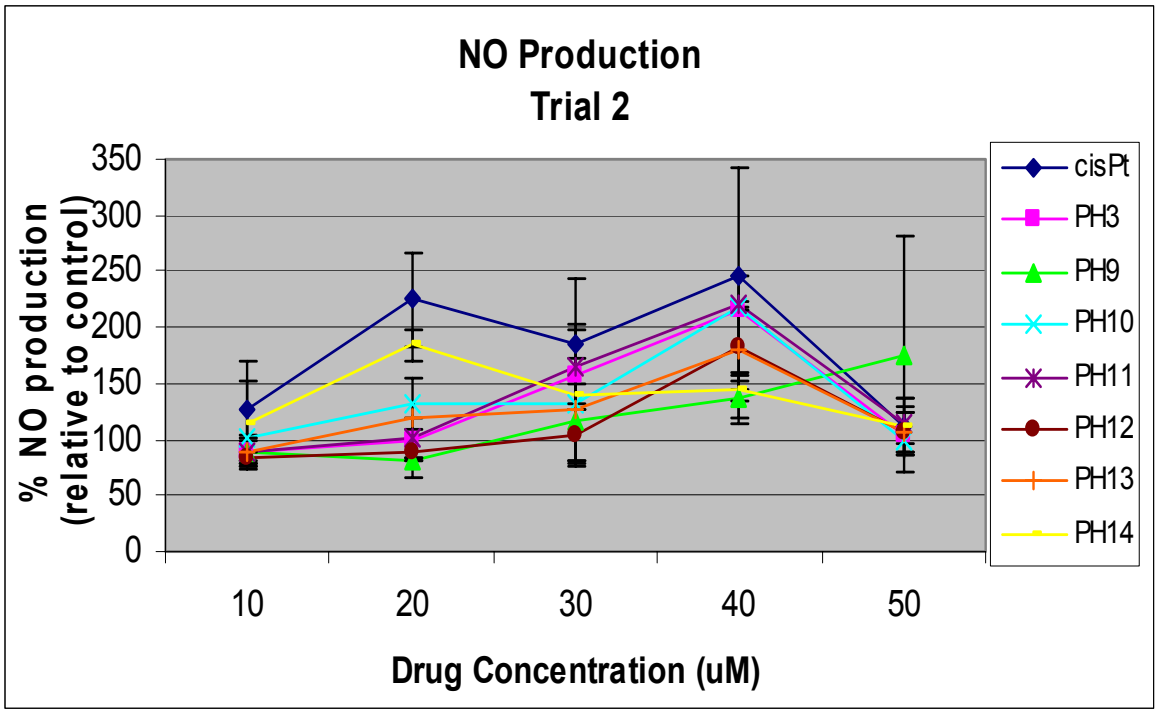

Figure 3.5C Trial 3 results of NO production.

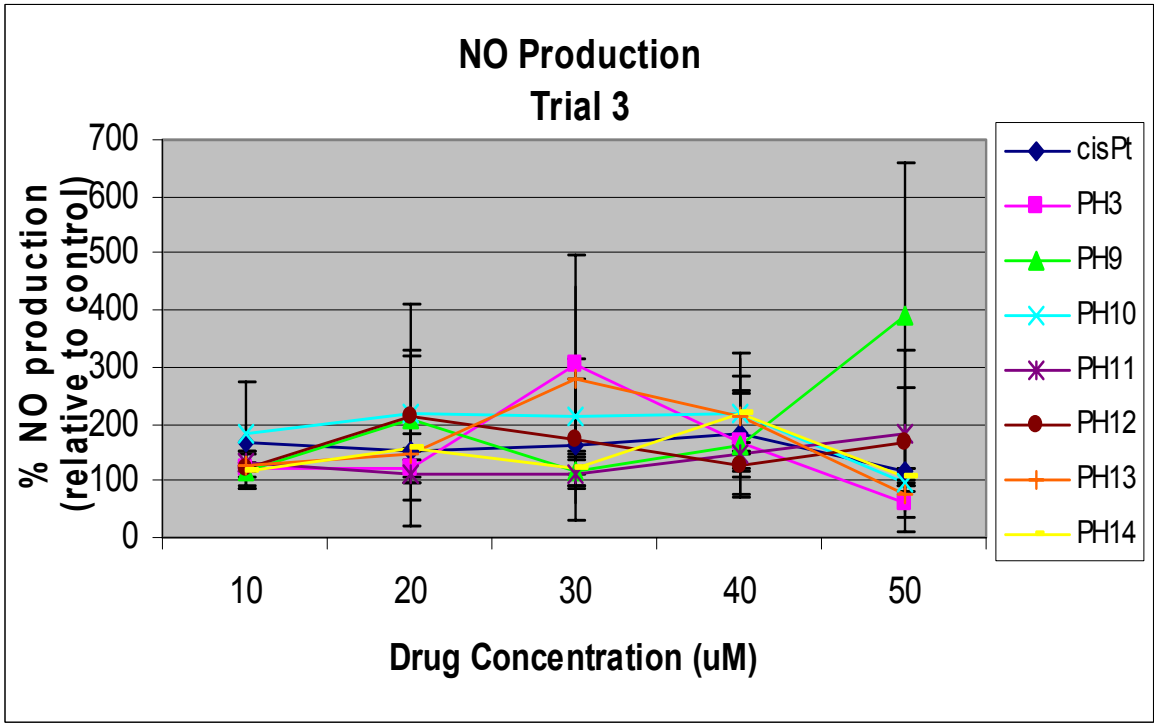

Figure 3.5D Trial 4 results of NO production from cells.

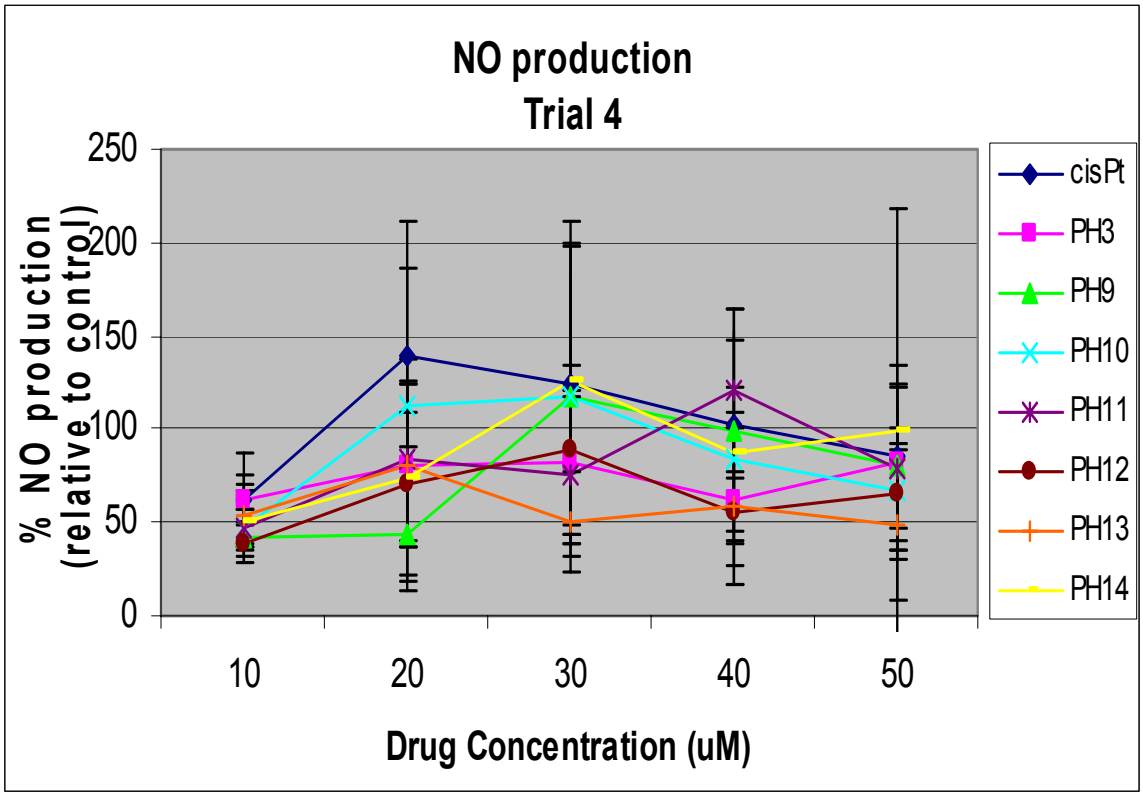

3.3 Nitric Oxide Synthase Expression

A Western blot analysis was performed to detect the expression of inducible nitric oxide synthase (iNOS) in treated and untreated cells. Figure 3.6 summarizes the relative iNOS expression (normalized to B-actin) after 48 hour treatment with PH compounds and cisplatin. All cells treated with PH compounds and cisplatin demonstrated higher iNOS values than control cells. iNOS is known to produce a high concentration of NO in tissues. Tumor cells that produce high levels of NO die *in vivo* [49]. Furthermore, studies have reported that an inverse relationship exists between the expression level of iNOS and the metastatic potential of murine tumor cells [48, 85-87].

These reports, in conjunction with our results, suggest that high levels of cellular NO production resulting from PH treatment may contribute to antitumor activity and decreased metastatic potential.

Figure 3.6 iNOS expression of PH treated cells.

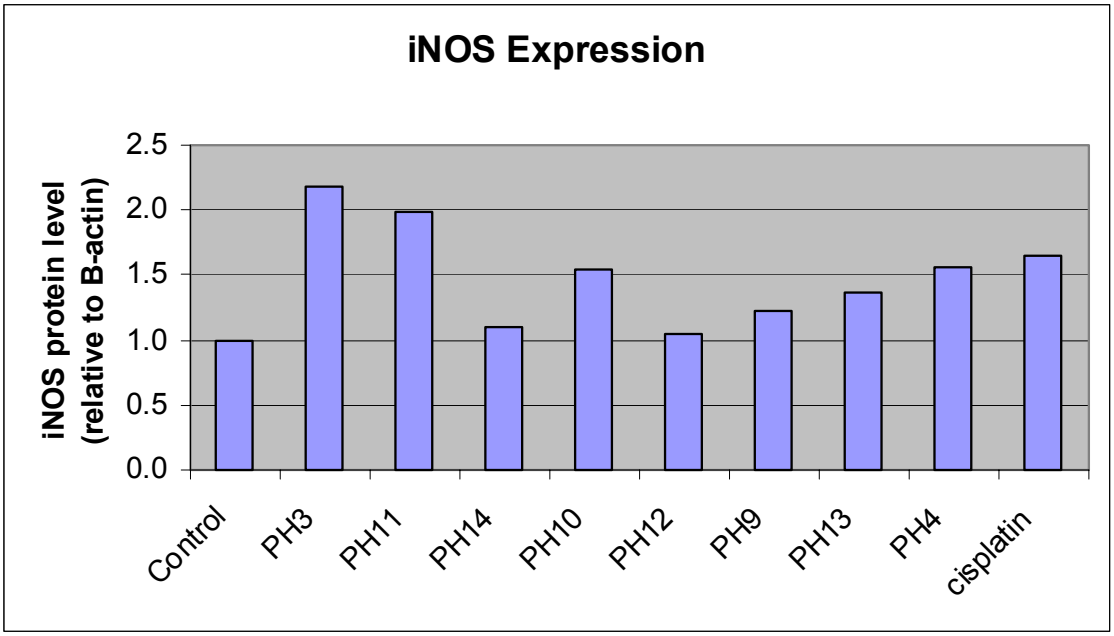

3.4 Toxicology

Due to mechanical errors, sample contamination, inconsistent collection practices, and reagent sensitivity, the blood serum data collected from the nude mice were deemed unreliable and thus excluded from analysis for this study. This decision was based on the generation of many negative values when assessing for blood enzymes, which is clearly erroneous. Toxicological profiles were thus developed from the animal groups from Yu et al.

Serum obtained at euthanasia was analyzed by the Vitros 950 automated chemical analyzer (Ortho Clinical Diagnostics). The biochemical profile of Mouse PH9-

1.1 from Day 1 was excluded from analysis due to a hemolyzed blood sample. C57BL6 mice from Day 1 showed the most abnormal blood chemistry values (Table 3.7). This was expected as these animals have the highest dose of drug in their bodies. As the drug is eliminated from their systems, the biochemical profiles of mice from Days 2-3 return

Table 3.7 Biochemical blood serum profiles for the assessment of toxicity.

		BUN	albumin	Creatinine	AST	ALT
	Normal	14-25	2.6-3.3	0.5-0.9	66-170	24-140
Day 1	Control 1.1	18.0	1.8	0.4	96.0	78.0
	Control 1.2	18.7	1.7	0.4	325.3	98.7
	Control 1.3	16.0	1.6	0.5	192.0	101.3
	PH9-1.1	60.8	1.3	1.0	339.2	224.0
	PH9-1.2	16.0	1.8	0.4	252.0	272.0
Day 2	Control 2.1	21.0	2.6	0.3	81.0	46.0
	Control 2.2	18.0	1.8	0.6	122.0	66.0
	Control 2.3	15.0	2.3	0.2	119.0	88.0
	PH9-2.1	20.0	1.6	0.4	78.0	76.0
	PH9-2.2	15.4	2.1	0.3	190.3	68.6
Day 3	Control 3.1	20.0	2.3	0.2	54.0	35.0
	Control 3.2	19.0	2.5	0.2	87.0	61.0
	PH9-3.1	18.0	2.3	0.2	161.0	70.0
	PH9-3.2	22.0	2.4	0.2	273.0	259.0
	PH9-3.3	20.0	1.9	0.2	84.0	44.0
	PH9-3.4	21.0	2.4	0.2	139.0	53.0
	PH9-3.5	14.0	2.3	0.2	347.0	101.0

closer to normal values. Normal ranges were determined from a variety of literature sources, so it should be noted that values will vary according to breed, age, sex, sampling technique, and quality of blood sample [88]. Therefore, interpretations are not definitive.

Blood urea nitrogen (BUN) and albumin levels are used to assess kidney function. Elevated BUN levels may indicate kidney failure, disease, and dehydration. Elevated albumin levels may indicate dehydration. Thus, if high albumin levels are noted in conjunction with other elevated values, it should be considered that the out-of-range

values are due to dehydration and not necessarily organ damage. Creatinine is the end product of phosphocreatine metabolism, an enzyme associated with muscle contractions. If elevated creatinine levels are observed with elevated BUN, kidney disease is often implicated.

Aspartate aminotransferase (AST) and alanine aminotransferase (ALT) levels are used to assess liver damage. AST is an indicator of the breakdown and elimination of nitrogen. Low AST levels may indicate starvation or malnutrition, while high levels may suggest liver damage, muscle damage, and inflammation. ALT is also involved with nitrogen metabolism and is most often associated with liver function. Low levels suggest starvation or malnutrition, while high levels indicate liver damage, toxin ingestion, and various metabolic disorders. Low creatinine levels indicate liver disease or starvation, while high levels may suggest dehydration, or kidney failure or disease.

Figure 3.6 graphically displays the biochemistry profiles of the blood collected from mice one day after the treatment injection. Although the control mice demonstrated individual blood chemistry values that may indicate toxicity, there was insufficient data across the various blood panels that could collectively suggest that there was any organ disease or damage. It is also evident that low albumin levels are observed for nearly all control and treated mice. One of albumin's functions is to transport drugs within the blood stream [89, 90]. It has been shown that albumin is reactive to platinum(II) complexes due to its thiol group [6]. Thus, low albumin levels may be anticipated with platinum treatment. Mouse PH9-1.2 had high levels of AST and ALT, and low albumin and creatinine. This finding may suggest that the administration of 5 mg/kg of PH9 to the animals may cause undesirable toxic side effects, and that a lower

Figure 3.7 Biochemical blood profiles of mice one day after 5 mg/kg drug injection.

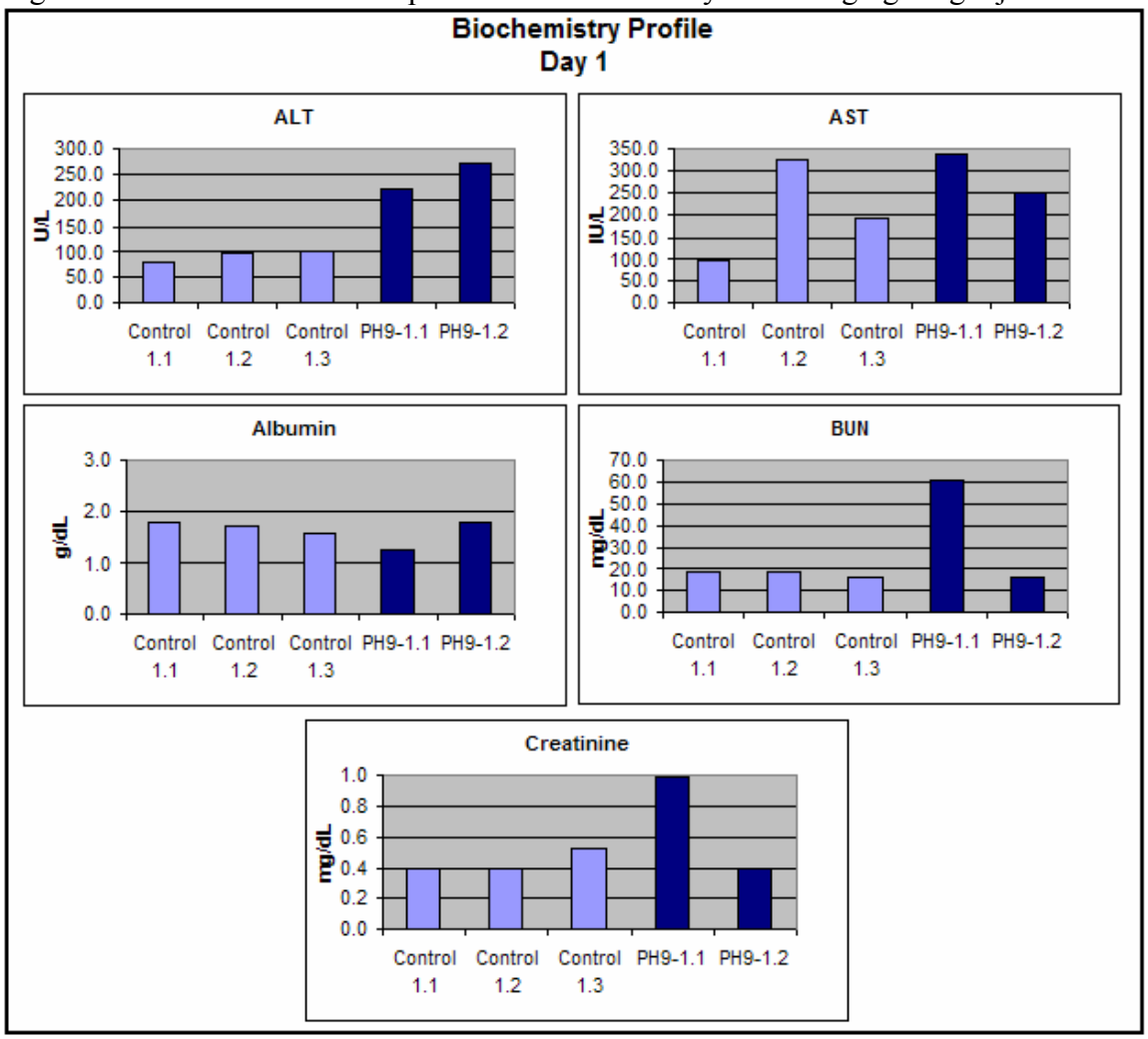

dose may need to be considered to prevent organ damage while sustaining the drug's anti-tumor action. Figure 3.8 displays the biochemistry profiles of the blood collected from mice two days after the last injection. Creatinine and albumin levels were again low for both treated and control mice, but other data did not support toxicity concerns. It was concluded that low creatinine levels were not suggestive of liver disease. However, the blood profile of PH9-2.2 of Day 2 demonstrates low creatinine and albumin in conjunction with high AST (but normal ALT), possibly indicative of liver damage.

Figure 3.8 Biochemical blood profiles of mice two days after 5 mg/kg drug injection.

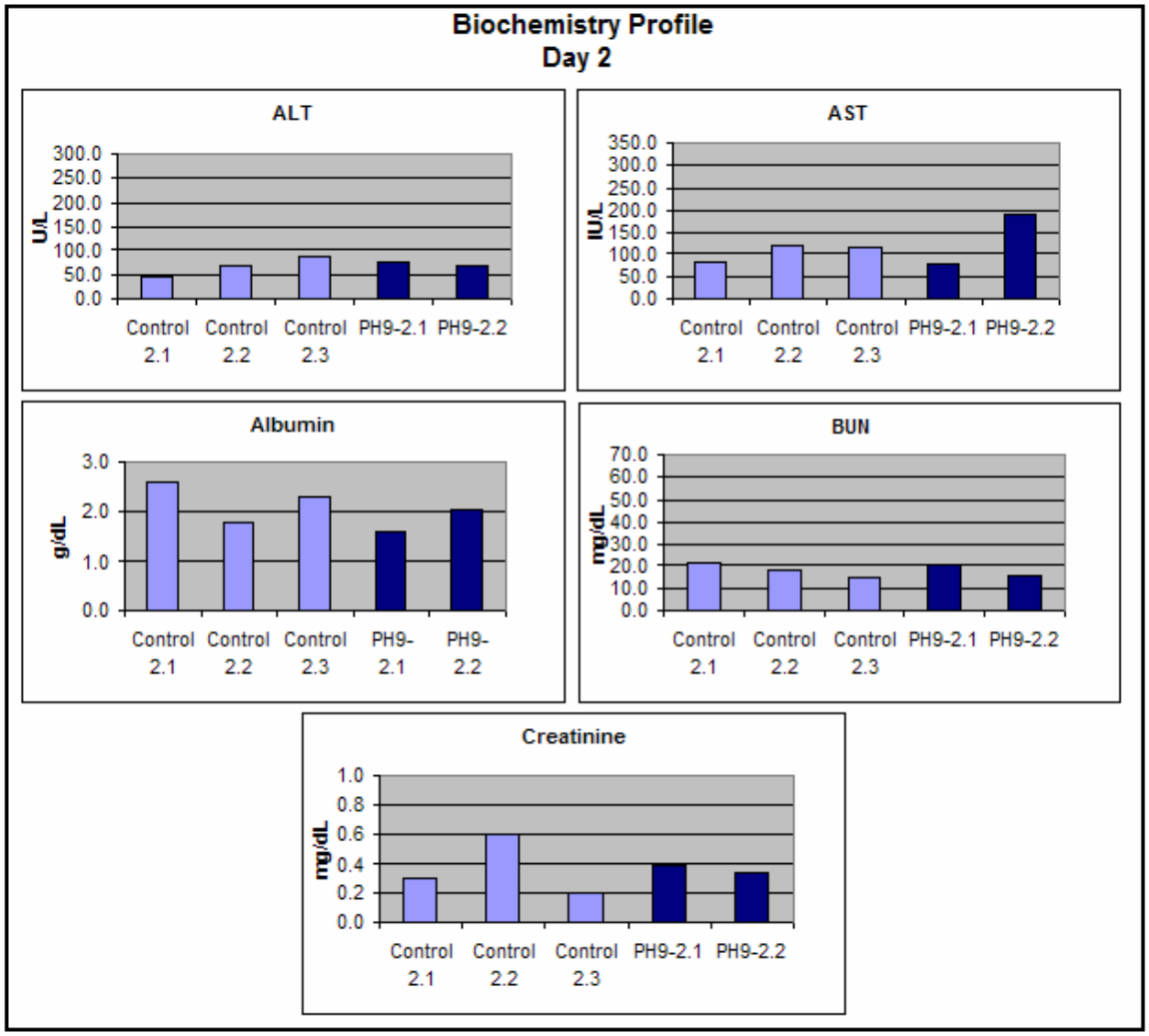

Figure 3.9 displays the biochemistry profiles of the blood collected from mice three days after the treatment injection. Again, only the data from the treated animals indicate possible liver toxicity. PH9-3.2 and PH9-3.5 had low values of creatinine and albumin, and high values of liver enzymes that suggested liver damage. The control animals did not exhibit overall signs of toxicity.

Figure 3.8 Biochemical blood profiles of mice three days after 5 mg/kg drug injection.

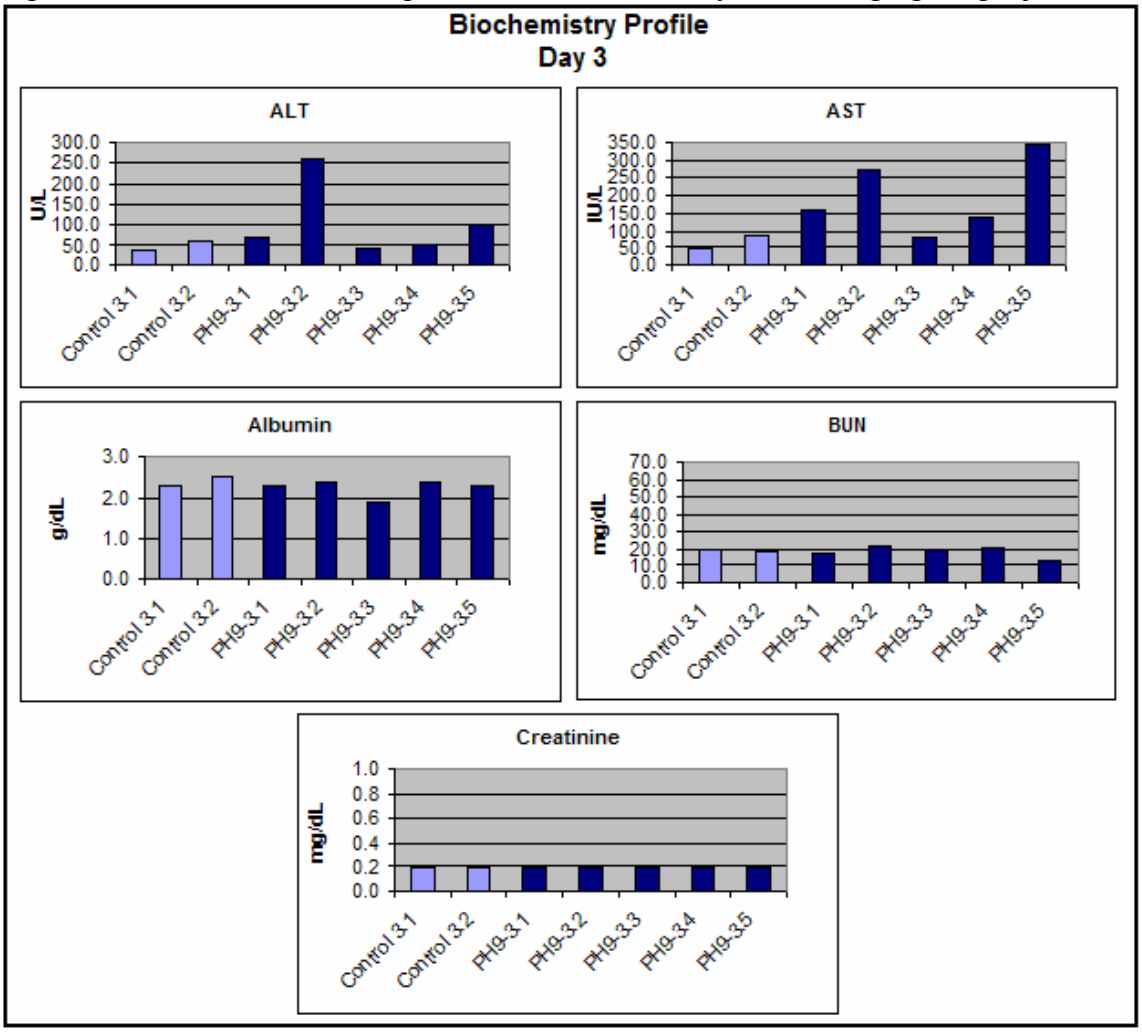

Cisplatin has been known for its induction of renal toxicity. Preclinical studies of cisplatin performed on mice reported that significant kidney damage was associated with the treatment [91, 92]. Leleiveld et al found levels of BUN and creatinine in cisplatin-treated C57BL mice (6.7-10.0 mg/kg) to be nearly five times the levels found in untreated animals on the fourth day after treatment [91]. These PH9 treated animals demonstrated no signs of nephrotoxicity. Table 3.8 compares our BUN

Table 3.8 Creatinine and BUN values of mice after cisplatin or PH9 treatment.

	BUN	Creatinine
Cisplatin	*nmol/L*	*Nmol/L*
Control	8.6 +/- 0.1	58.5 +/- 0.6
6.7 mg/kg cisplatin	55.0 +/- 15.0	281.0 +/- 88.0
10.0 mg/kg cisplatin	72.0 +/- 12.0	282.0 +/- 55.0
PH9	*mg/Dl*	*mg/dL*
Control	18.2 +/- 2.0	0.4 +/- 0.2
5 mg/kg PH9	18.3 +/- 2.9	0.3 +/- 0.1

and creatinine values with those values reported from cisplatin. It is evident that PH9 treated mice did not exhibit any measurable signs of kidney disease. Values of the treated animals are similar to values of untreated animals. This evidence suggests that PH9 may reduce toxicity relative to cisplatin.

3.5 X-Ray Diffraction

X-ray analysis of the platinum-treated cell block from the TEM was unable detect a platinum signal anywhere in the cells. A spectra generated from the positive-platinum control confirmed that the x-ray detector was functional. Energy emission signals from the analysis of treated cells showed the presence of sulfur, phosphorus and chlorine cells. The emission spectra also indicated the presence of silica in the resin.

X-ray analysis of the platinum-treated bulk sample from the SEM was unable to detect a platinum signal anywhere in the cells. Analysis of the fixative and the drug also suggested that there was no platinum in the sample.

This data indicates that the level of platinum in the cells and culture medium after treatment and fixation was below the minimum level of detectability for the

x-ray analyzer. Another mode of analysis with lower limits of detection that may be more sensitive may be necessary to detect and quantify the amount of platinum present in the cells. Alternatively, platinum localization may require the analysis of cellular organelles though the lysis of large numbers of treated cells. This may be mediated by atomic absorption or inductively-coupled plasma.

3.6 Inhibition of STAT Dimerization

The PH compounds were able to inhibit acellular dimerization of STAT proteins at concentrations as low as 0.3 uM. At concentrations of 30 uM, complete inhibition of STAT dimerization was observed for all PH compounds. The IC_{50} for STAT dimers by these compounds are summarized in Table 3.9.

Table 3.9 Calculated IC50 values of PH compounds for STAT dimerization.

Compound	STAT3:STAT3 (uM)	STAT1:STAT3 (uM)	STAT1:STAT1(uM)
PH4	0.5	1.0	1.0
PH1	0.5	1.0	1.0
PH10	2.0	2.2	0.5
PH7	0.4	0.4	0.4
PH11	0.3	0.4	0.4

Previous studies with other inhibitors of STAT report that much higher concentrations are necessary to achieve the same effect. Blaskovich et al found that JSI-124 (Ccurbitacin I) had an IC_{50} value of 500 nm in the human lung carcinoma A549 cell line [93]. Grandis et al used antisense oligonucleotides to inhibit STAT at 12.5 uM. It is evident that the IC_{50} values of the PH compounds are effective at lower concentrations, suggesting that these PH compounds may be superior STAT inhibitors. However, since

this assay was conducted with nuclear extracts and not whole cells, cellular transport and other mechanisms and other mechanisms will activities *in vivo.*

Figure 3.10 Inhibition of STAT dimerization by PH compounds.

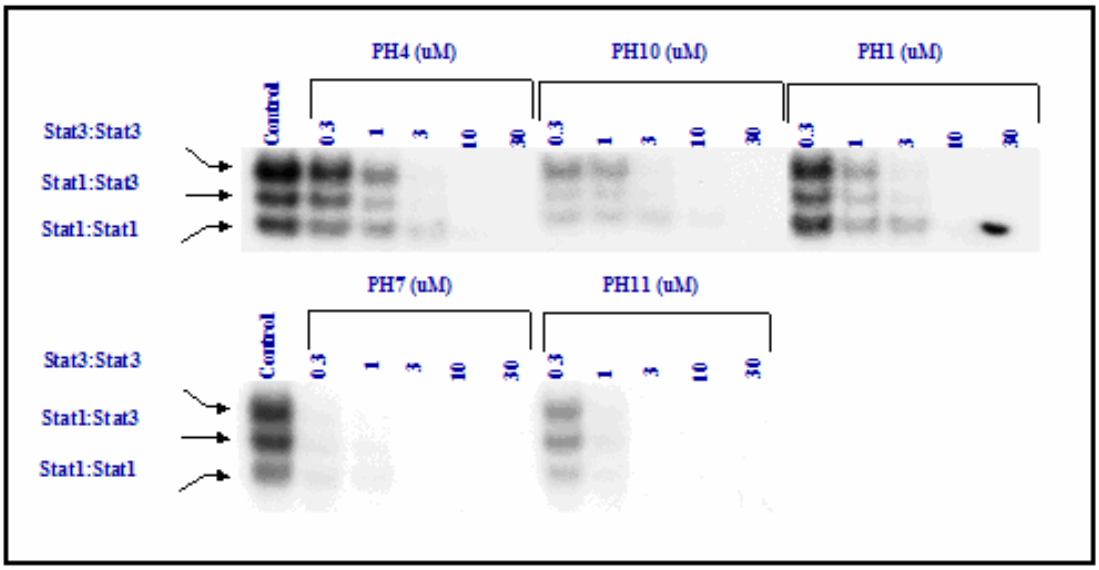

Assessment of the effects of the PH compounds on other STAT dimers is critical in understanding the compounds' effects on other signaling cascades. Though the PH compounds were effective at preventing STAT3:STAT3 binding, the STAT1 homodimer is less affected at concentrations below 10 uM (Figure 3.10). It has been shown that STAT1 activation is elevated in a few cancers, but its function has mostly been observed as growth suppression rather than malignant transformation [94] . Thus, the preservation of the STAT1 dimerization function is desirable in maintaining its actions as a potential tumor suppressor. The STAT1:STAT3 heterodimer has been weakly linked to similar effects of constitutively active STAT3, so its inhibition continues to be a desired effect.

3.7 Angiogenesis

As shown in Figure 3.11, Yu's group at Moffitt revealed that Western Blot analysis of cells treated with PH9 resulted in decreased HIF-1α and VEGF expression. Lanes 1-4 denote the concentration of PH9 administered. B-actin is a housekeeping gene

Figure 3.11 Determination of HIF-1α, VEGF, and STAT3 expression by Western blot. PH9 affects HIF-1α and VEGF expression in a dose-dependent manner (top gel). This reduction of expression can be correlated with STAT3 expression (bottom gel).

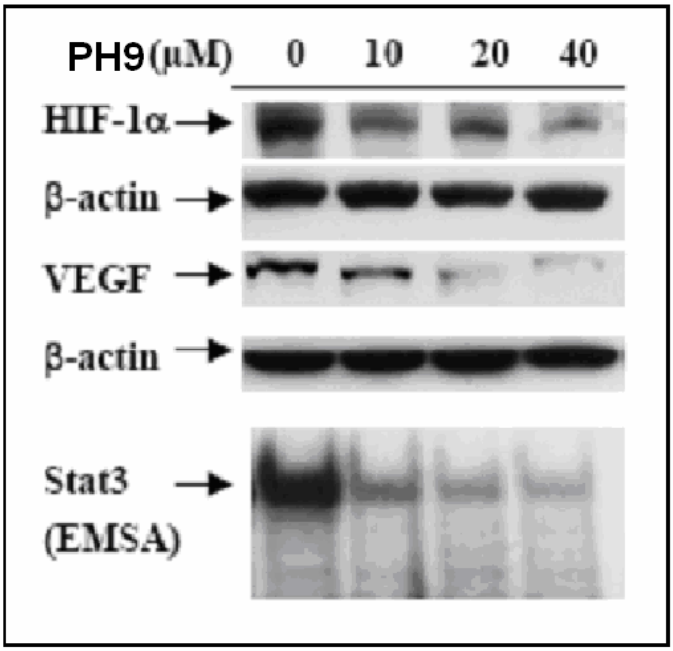

that normalizes the amount of protein in each well to maintain consistency for analysis between lanes. The intensity of HIF-1α and VEGF bands fades across the lanes, indicating that PH9 affects the expression of these proteins in a dose-dependent manner. This reduction in expression of HIF-1α and VEGF correlates with the expression of STAT3, suggesting a relationship. As STAT3 expression decreases, HIF-1α and VEGF expression decreases as well. This data is in agreement with the data found in section

3.7, where PH9 was found to reduce STAT3 activity. Since the over-expression of VEGF and HIF-1α is associated with tumor angiogenesis, tumor cell proliferation and invasion, PH9 may be an inhibitor of critical angiogenic proteins, possibly related to STAT3 inhibition.

Further *in vivo* studies verified that treatment the blocking with PH9 resulted in reduced microvessel density. Matrigel-implanted human breast carcinoma MCF-7 tumors from PH treated mice were excised and analyzed for angiogenesis.

Figure 3.12 Matrigel plugs of MCF-7 tumors.

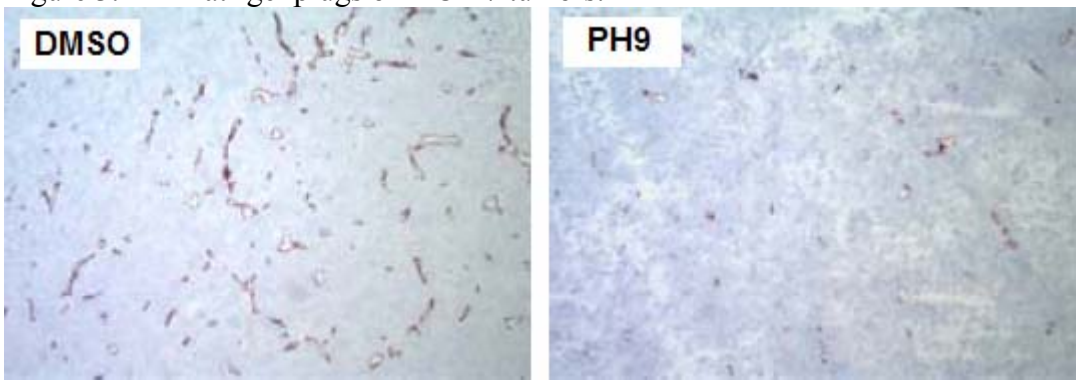

Figure 3.12 shows control and PH9 treated Matrigel plugs of MCF-7 tumors that were harvested 5 days after implantation. Mice treated with the DMSO vehicle demonstrate increased neovasculature as compared to mice treated with PH9. Further studies identifying mechanistic pathways are in progress in collaborations with the Yu lab.

3.8 Tumor Growth Inhibition

In vitro studies conducted by Yu's group indicated that MB49 cells did not respond to PH9 treatment [95]. However, mice treated with PH9 demonstrated inhibited

MB49-tumor growth. Within 5 days of tumor induction, a palpable mass was detected for control and experimental mice. Tumors continued to grow throughout the drug

Figure 3.13 Tumor size (mm^3) of control and PH treated mice.

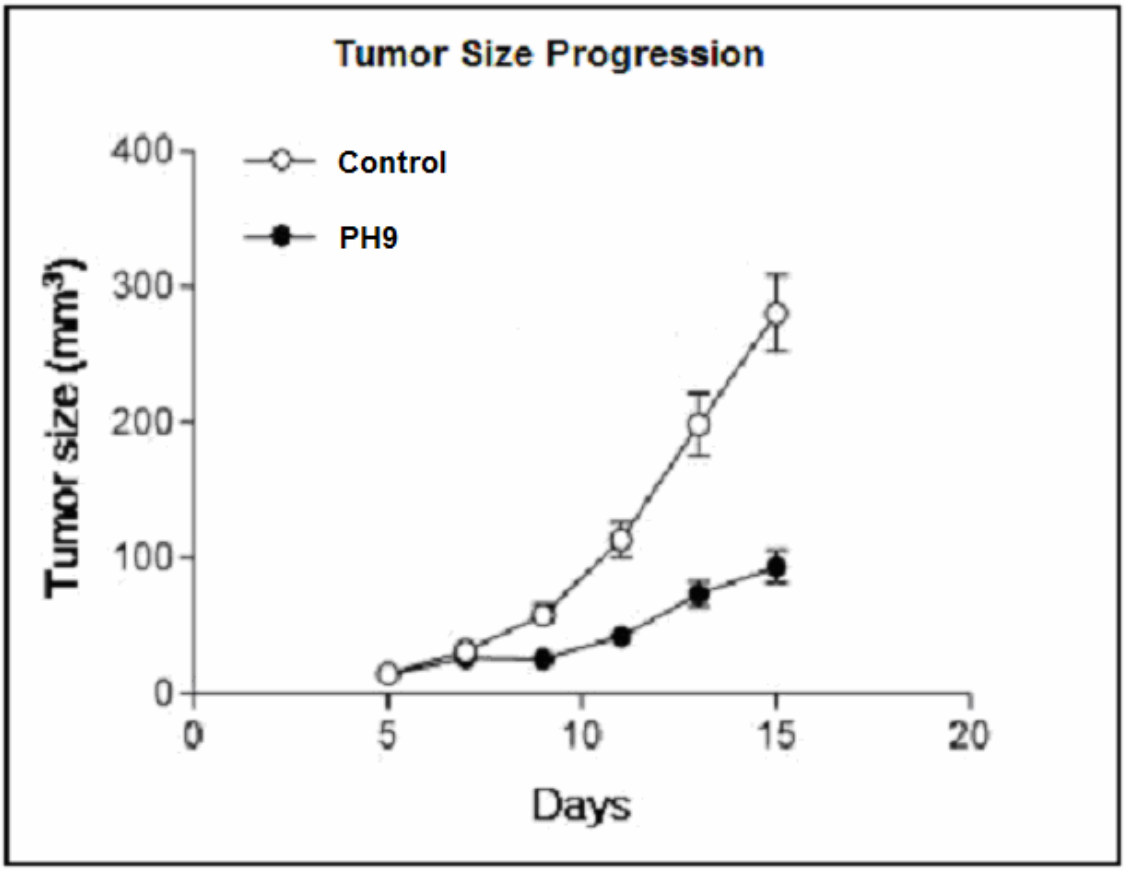

regimen for both groups. Animals treated with PH9 exhibited significantly slower growth and smaller tumors as compared with control animals (Figure 3.13). Because the same cell line used in vitro did not respond to PH9 treatment, it is believed that the tumor inhibition was due to an immunological or systemic response to the drug. These facts suggest that PH9 may be used as an effective chemotherapeutic agent to inhibit tumor growth.

CHAPTER 4: CONCLUSION

In an effort to overcome common problems associated with the traditional methods of cisplatin cancer treatment, we have synthesized novel chemotherapeutic agents designed to circumvent drug-resistance and toxic side effects, while achieving improved activity by targeting unique pathways unique to cancer. We focused on obtaining preliminary data to characterize these compounds in order to elucidate potential compounds for further study. *In vitro* and *in vivo* studies were performed to describe their activities.

Table 4.1 summarizes the results of key assays performed on the PH compounds. Data not shown in this table include toxicity and angiogenesis findings, since only PH9 was examined in those assays. Cell proliferation assays performed from XTT and MTT tetrazolium salt reagents showed that all PH compounds, with the exception of PH12 and PH13, exhibited lower IC50 values than that of cisplatin. Western blot analyses of iNOS expression demonstrated that PH3 and PH11 treated cells had greater iNOS expression than cisplatin. All compounds that were tested for inhibition of STAT3 dimerization had IC50 values of 2 uM or lower. Contrary to the nephrotoxicity commonly observed in cisplatin-treated mice, our toxicological analysis of PH9 treated mice indicated that no kidney damage was evident. However, elevated livr enzymes were measured, warranting further studies. Additionally, PH9 exhibited anti-

Table 4.1 Comparison of the results of various assays on PH compounds.

Compound	Avg IC50 (uM)	Relative iNOS expression	STAT3 IC50 (uM)
Cisplatin	65.3 +/- 12.1	1.64	----
PH1	41.7 +/- 7.9	----	0.5
PH2	44.5 +/- 3.5	----	----
PH3	58.0 +/- 22.6	2.19	----
PH4	61.8 +/- 11.1	1.56	0.5
PH5	43	----	----
PH6	46	----	----
PH7	54.5 +/- 6.5	----	0.4
PH8	276.5 +/- 229.5	----	----
PH9	211 +/- 236.2	1.23	----
PH10	52.3 +/- 4.6	1.55	2.0
PH11	52.0 +/- 3.7	1.99	0.3
PH12	191	----	----
PH13	107	1.37	----
PH14	58	1.10	----

angiogenesis properties, as demonstrated by the inhibition of HIF-1α and VEGF expression. These assays have identified PH3, PH9, and PH11 as the most promising candidates for further studies.

These nitroplatinum(IV) compounds are also expected to circumvent the resistance seen with cisplatin since their novel mechanisms may not involve DNA binding and therefore evades the DNA mismatch repair mechanism. These data suggest that these novel nitroplatinum compounds may serve as effective alternatives to cisplatin.

Further studies will refine the data established in this study. Future work will include the determination of the spectrum of activity of the PH compounds in various cell lines. We also hope to identify the optimal dose by conducting further cell viability assays and toxicology studies. Additionally, the structures of the platinum complexes must be verified using x-ray crystallography. Nitric oxide production may be assessed with further Western blotting for iNOS. Lastly, we wish to explore STAT3 inhibition

and anti-angiogenesis mechanisms for PH3 and PH11. This additional work may reveal future directions into clinical trials.

References

1 Baquiran DC GJ. *Lippincott's Cancer Chemotherapy Handbook*, Lippincott. 1998.

2 Kwon YE, Whang KJ, Park YJ*, et al.* (2003). Synthesis, characterization and antitumor activity of novel octahedral Pt(IV) complexes. Bioorg Med Chem 11:1669-1676.

3 Jamieson ER and Lippard SJ. (1999). Structure, Recognition, and Processing of Cisplatin-DNA Adducts. Chem Rev 99:2467-2498.

4 Barnes KR, Kutikov A and Lippard SJ. (2004). Synthesis, characterization, and cytotoxicity of a series of estrogen-tethered platinum(IV) complexes. Chem Biol 11:557-564.

5 Cohen SM and Lippard SJ. (2001). Cisplatin: from DNA damage to cancer chemotherapy. Prog Nucleic Acid Res Mol Biol 67:93-130.

6 Dolman RC, Deacon GB and Hambley TW. (2002). Studies of the binding of a series of platinum(IV) complexes to plasma proteins. J Inorg Biochem 88:260-267.

7 Zak F, Turanek J, Kroutil A*, et al.* (2004). Platinum(IV) complex with adamantylamine as nonleaving amine group: synthesis, characterization, and in vitro antitumor activity against a panel of cisplatin-resistant cancer cell lines. J Med Chem 47:761-763.

8 Song R, Park SY, Kim YS*, et al.* (2003). Synthesis and cytotoxicity of new platinum(IV) complexes of mixed carboxylates. J Inorg Biochem 96:339-345.

9 Rixe O, Ortuzar W, Alvarez M*, et al.* (1996). Oxaliplatin, tetraplatin, cisplatin, and carboplatin: spectrum of activity in drug-resistant cell lines and in the cell lines of the National Cancer Institute's Anticancer Drug Screen panel. Biochem Pharmacol 52:1855-1865.

10 Siddik ZH. (2003). Cisplatin: mode of cytotoxic action and molecular basis of resistance. Oncogene 22:7265-7279.

11 Toshimitsu H, Hashimoto K, Tangoku A*, et al.* (2004). Molecular signature linked to acquired resistance to cisplatin in esophageal cancer cells. Cancer Lett 211:69-78.

12 Brockman RW. (1963). Mechanisms of Resistance to Anticancer Agents. Adv Cancer Res 57:129-234.

13 Haber DA, Beverley SM, Kiely ML*, et al.* (1981). Properties of an altered dihydrofolate reductase encoded by amplified genes in cultured mouse fibroblasts. J Biol Chem 256:9501-9510.

14 Perez RP. (1998). Cellular and molecular determinants of cisplatin resistance. Eur J Cancer 34:1535-1542.

15 Lage H and Dietel M. (1999). Involvement of the DNA mismatch repair system in antineoplastic drug resistance. J Cancer Res Clin Oncol 125:156-165.

16 Aebi S, Kurdi-Haidar B, Gordon R*, et al.* (1996). Loss of DNA mismatch repair in acquired resistance to cisplatin. Cancer Res 56:3087-3090.

17 Fink D, Zheng H, Nebel S*, et al.* (1997). In vitro and in vivo resistance to cisplatin in cells that have lost DNA mismatch repair. Cancer Res 57:1841-1845.

18 Anthoney DA, McIlwrath AJ, Gallagher WM*, et al.* (1996). Microsatellite instability, apoptosis, and loss of p53 function in drug-resistant tumor cells. Cancer Res 56:1374-1381.

19 Hartmann JT and Lipp HP. (2003). Toxicity of platinum compounds. Expert Opin Pharmacother 4:889-901.

20 Pendyala L, Cowens JW, Chheda GB*, et al.* (1988). Identification of cis-dichloro-bis-isopropylamine platinum(II) as a major metabolite of iproplatin in humans. Cancer Res 48:3533-3536.

21 Novakova O, Vrana O, Kiseleva VI*, et al.* (1995). DNA interactions of antitumor platinum(IV) complexes. Eur J Biochem 228:616-624.

22 Kelland LR. (2000). An update on satraplatin: the first orally available platinum anticancer drug. Expert Opin Investig Drugs 9:1373-1382.

23 O'Rourke TJ, Weiss GR, New P*, et al.* (1994). Phase I clinical trial of ormaplatin (tetraplatin, NSC 363812). Anticancer Drugs 5:520-526.

24 Hurwitz HI. (2004). Introduction: targeting angiogenesis in cancer therapy. Oncologist 9 Suppl 1:1.

25 Stoeltzing O, McCarty MF, Wey JS*, et al.* (2004). Role of hypoxia-inducible factor 1alpha in gastric cancer cell growth, angiogenesis, and vessel maturation. J Natl Cancer Inst 96:946-956.

26 Jiang BH, Agani F, Passaniti A*, et al.* (1997). V-SRC induces expression of hypoxia-inducible factor 1 (HIF-1) and transcription of genes encoding vascular endothelial growth factor and enolase 1: involvement of HIF-1 in tumor progression. Cancer Res 57:5328-5335.

27 Laughner E, Taghavi P, Chiles K*, et al.* (2001). HER2 (neu) signaling increases the rate of hypoxia-inducible factor 1alpha (HIF-1alpha) synthesis: novel mechanism for HIF-1-mediated vascular endothelial growth factor expression. Mol Cell Biol 21:3995-4004.

28 Semenza GL. (2003). Targeting HIF-1 for cancer therapy. Nat Rev Cancer 3:721-732.

29 Inoue M, Hager JH, Ferrara N*, et al.* (2002). VEGF-A has a critical, nonredundant role in angiogenic switching and pancreatic beta cell carcinogenesis. Cancer Cell 1:193-202.

30 Huss WJ, Barrios RJ and Greenberg NM. (2003). SU5416 selectively impairs angiogenesis to induce prostate cancer-specific apoptosis. Mol Cancer Ther 2:611-616.

31 Benjamin LE, Golijanin D, Itin A*, et al.* (1999). Selective ablation of immature blood vessels in established human tumors follows vascular endothelial growth factor withdrawal. J Clin Invest 103:159-165.

32 Bromberg J and Darnell JE, Jr. (2000). The role of STATs in transcriptional control and their impact on cellular function. Oncogene 19:2468-2473.

33 Darnell JE, Jr. (1998). Studies of IFN-induced transcriptional activation uncover the Jak-Stat pathway. J Interferon Cytokine Res 18:549-554.

34 Darnell JE, Jr., Kerr IM and Stark GR. (1994). Jak-STAT pathways and transcriptional activation in response to IFNs and other extracellular signaling proteins. Science 264:1415-1421.

35 Decker T and Kovarik P. (1999). Transcription factor activity of STAT proteins: structural requirements and regulation by phosphorylation and interacting proteins. Cell Mol Life Sci 55:1535-1546.

36 Schindler C and Brutsaert S. (1999). Interferons as a paradigm for cytokine signal transduction. Cell Mol Life Sci 55:1509-1522.

37 Darnell JE, Jr. (1997). STATs and gene regulation. Science 277:1630-1635.

38 Buettner R, Mora LB and Jove R. (2002). Activated STAT signaling in human tumors provides novel molecular targets for therapeutic intervention. Clin Cancer Res 8:945-954.

39 Benekli M, Baer MR, Baumann H*, et al.* (2003). Signal transducer and activator of transcription proteins in leukemias. Blood 101:2940-2954.

40 Shi Q, Huang S, Jiang W*, et al.* (1999). Direct correlation between nitric oxide synthase II inducibility and metastatic ability of UV-2237 murine fibrosarcoma cells carrying mutant p53. Cancer Res 59:2072-2075.

41 Lepoivre M, Flaman JM, Bobe P*, et al.* (1994). Quenching of the tyrosyl free radical of ribonucleotide reductase by nitric oxide. Relationship to cytostasis induced in tumor cells by cytotoxic macrophages. J Biol Chem 269:21891-21897.

42 Stein CS, Fabry Z, Murphy S*, et al.* (1995). Involvement of nitric oxide in IFN-gamma-mediated reduction of microvessel smooth muscle cell proliferation. Mol Immunol 32:965-973.

43 Mahoney KH and Heppner GH. (1987). FACS analysis of tumor-associated macrophage replication: differences between metastatic and nonmetastatic murine mammary tumors. J Leukoc Biol 41:205-211.

44 Yim CY, Bastian NR, Smith JC*, et al.* (1993). Macrophage nitric oxide synthesis delays progression of ultraviolet light-induced murine skin cancers. Cancer Res 53:5507-5511.

45 Beckman JS, Beckman TW, Chen J*, et al.* (1990). Apparent hydroxyl radical production by peroxynitrite: implications for endothelial injury from nitric oxide and superoxide. Proc Natl Acad Sci U S A 87:1620-1624.

46 Wink DA, Feelisch M, Fukuto J*, et al.* (1998). The cytotoxicity of nitroxyl: possible implications for the pathophysiological role of NO. Arch Biochem Biophys 351:66-74.

47 Lin KT, Xue JY, Sun FF*, et al.* (1997). Reactive oxygen species participate in peroxynitrite-induced apoptosis in HL-60 cells. Biochem Biophys Res Commun 230:115-119.

48 Xie K and Fidler IJ. (1998). Therapy of cancer metastasis by activation of the inducible nitric oxide synthase. Cancer Metastasis Rev 17:55-75.

49 Trikha P, Sharma N and Athar M. (2001). Nitroglycerin: a NO donor inhibits TPA-mediated tumor promotion in murine skin. Carcinogenesis 22:1207-1211.

50 Drapier JC and Hibbs JB, Jr. (1986). Murine cytotoxic activated macrophages inhibit aconitase in tumor cells. Inhibition involves the iron-sulfur prosthetic group and is reversible. J Clin Invest 78:790-797.

51 Lepoivre M, Fieschi F, Coves J*, et al.* (1991). Inactivation of ribonucleotide reductase by nitric oxide. Biochem Biophys Res Commun 179:442-448.

52 Wharton M, Granger DL and Durack DT. (1988). Mitochondrial iron loss from leukemia cells injured by macrophages. A possible mechanism for electron transport chain defects. J Immunol 141:1311-1317.

53 Lauder I, Aherne W, Stewart J*, et al.* (1977). Macrophage infiltration of breast tumours: a prospective study. J Clin Pathol 30:563-568.

54 Underwood JC. (1974). Lymphoreticular infiltration in human tumours: prognostic and biological implications: a review. Br J Cancer 30:538-548.

55 Hibbs JB, Jr., Taintor RR, Vavrin Z*, et al.* (1988). Nitric oxide: a cytotoxic activated macrophage effector molecule. Biochem Biophys Res Commun 157:87-94.

56 Marletta MA, Yoon PS, Iyengar R*, et al.* (1988). Macrophage oxidation of L-arginine to nitrite and nitrate: nitric oxide is an intermediate. Biochemistry 27:8706-8711.

57 Stuehr DJ and Nathan CF. (1989). Nitric oxide. A macrophage product responsible for cytostasis and respiratory inhibition in tumor target cells. J Exp Med 169:1543-1555.

58 Wink DA, Cook JA, Christodoulou D*, et al.* (1997). Nitric oxide and some nitric oxide donor compounds enhance the cytotoxicity of cisplatin. Nitric Oxide 1:88-94.

59 Azizzadeh B, Yip HT, Blackwell KE*, et al.* (2001). Nitric oxide improves cisplatin cytotoxicity in head and neck squamous cell carcinoma. Laryngoscope 111:1896-1900.

60 Cook JA, Krishna MC, Pacelli R*, et al.* (1997). Nitric oxide enhancement of melphalan-induced cytotoxicity. Br J Cancer 76:325-334.

61 Adams DJ, Levesque MC, Weinberg JB*, et al.* (2001). Nitric oxide enhancement of fludarabine cytotoxicity for B-CLL lymphocytes. Leukemia 15:1852-1859.

62 Mitchell JB, Cook JA, Krishna MC*, et al.* (1996). Radiation sensitisation by nitric oxide releasing agents. Br J Cancer Suppl 27:S181-184.

63 Rosenberg B. (1985). Fundamental studies with cisplatin. Cancer 55:2303-l2306.

64 Andrews PA and Howell SB. (1990). Cellular pharmacology of cisplatin: perspectives on mechanisms of acquired resistance. Cancer Cells 2:35-43.

65 Ozols RF and Young RC. (1984). Chemotherapy of ovarian cancer. Semin Oncol 11:251-263.

66 Kelley SL and Rozencweig M. (1989). Resistance to platinum compounds: mechanisms and beyond. Eur J Cancer Clin Oncol 25:1135-1140.

67 Putnam KP, Bombick DW and Doolittle DJ. (2002). Evaluation of eight in vitro assays for assessing the cytotoxicity of cigarette smoke condensate. Toxicol In Vitro 16:599-607.

68 Reedijk J. (1999). Why does Cisplatin reach Guanine-n7 with competing s-donor ligands available in the cell? Chem Rev 99:2499-2510.

69 Nooter K and Stoter G. (1996). Molecular mechanisms of multidrug resistance in cancer chemotherapy. Pathol Res Pract 192:768-780.

70 Kojima H, Nakatsubo N, Kikuchi K*, et al.* (1998). Detection and imaging of nitric oxide with novel fluorescent indicators: diaminofluoresceins. Anal Chem 70:2446-2453.

71 Itoh Y, Ma FH, Hoshi H*, et al.* (2000). Determination and bioimaging method for nitric oxide in biological specimens by diaminofluorescein fluorometry. Anal Biochem 287:203-209.

72 Molecular Probes. (2001). Product Information Sheet. Nitric Oxide Indicators: DAF-FM and DAF-FM Diacetate.

73 Goodwin BL, Solomonson LP and Eichler DC. (2004). Argininosuccinate synthase expression is required to maintain nitric oxide production and cell viability in aortic endothelial cells. J Biol Chem 279:18353-18360.

74 Turkson J, Ryan D, Kim JS*, et al.* (2001). Phosphotyrosyl peptides block Stat3-mediated DNA binding activity, gene regulation, and cell transformation. J Biol Chem 276:45443-45455.

75 Niu G, Heller R, Catlett-Falcone R*, et al.* (1999). Gene therapy with dominant-negative Stat3 suppresses growth of the murine melanoma B16 tumor in vivo. Cancer Res 59:5059-5063.

76 Molecular Probes. (2002). Product Information Sheet. Amplex Red Glucose/Glucose Oxidase Assay Kit (A-22189).

77 Molecular Probes. (2002). Product Information Sheet. Amplex Red Glutamic Acid/Glutamate Oxidase Assay Kit (A-12221).

78 Amresco. (2000). Technical Bulletin. Albumin Reagent.

79 Amresco. (2000). Technical Bulletin. ALT Reagent.

80 Amresco. (2000). Technical Bulletin. BUN Reagent.

81 Niu G, Wright KL, Huang M*, et al.* (2002). Constitutive Stat3 activity up-regulates VEGF expression and tumor angiogenesis. Oncogene 21:2000-2008.

82 Garcia-Lopez P, Rodriguez-Dorantes M, Perez-Cardenas E*, et al.* (2004). Synergistic effects of ICI 182,780 on the cytotoxicity of cisplatin in cervical carcinoma cell lines. Cancer Chemother Pharmacol 53:533-540.

83 Turanek J, Kasna A, Zaluska D*, et al.* (2004). New platinum(IV) complex with adamantylamine ligand as a promising anti-cancer drug: comparison of in vitro cytotoxic potential towards A2780/cisR cisplatin-resistant cell line within homologous series of platinum(IV) complexes. Anticancer Drugs 15:537-543.

84 Galanski M, Arion VB, Jakupec MA*, et al.* (2003). Recent developments in the field of tumor-inhibiting metal complexes. Curr Pharm Des 9:2078-2089.

85 Xie K, Bielenberg D, Huang S*, et al.* (1997). Abrogation of tumorigenicity and metastasis of murine and human tumor cells by transfection with the murine IFN-beta gene: possible role of nitric oxide. Clin Cancer Res 3:2283-2294.

86 Xie K, Dong Z and Fidler IJ. (1996). Activation of nitric oxide synthase gene for inhibition of cancer metastasis. J Leukoc Biol 59:797-803.

87 Xie K, Huang S, Dong Z*, et al.* (1995). Transfection with the inducible nitric oxide synthase gene suppresses tumorigenicity and abrogates metastasis by K-1735 murine melanoma cells. J Exp Med 181:1333-1343.

88 Brij M. Mitruka HMR. *Clinical Biochemical and Hematological Reference Values in Normal Experimental Animals and Normal Humans*, 2. Masson Pub. USA. 1981.
89 Peters T, Jr. (1985). Serum albumin. Adv Protein Chem 37:161-245.

90 Takahashi I, Ohnuma T, Kavy S*, et al.* (1980). Interaction of human serum albumin with anticancer agents in vitro. Br J Cancer 41:602-608.

91 Lelieveld P, Van der Vijgh WJ, Veldhuizen RW*, et al.* (1984). Preclinical studies on toxicity, antitumour activity and pharmacokinetics of cisplatin and three recently developed derivatives. Eur J Cancer Clin Oncol 20:1087-1104.

92 Townsend DM, Deng M, Zhang L*, et al.* (2003). Metabolism of Cisplatin to a nephrotoxin in proximal tubule cells. J Am Soc Nephrol 14:1-10.

93 Blaskovich MA, Sun J, Cantor A*, et al.* (2003). Discovery of JSI-124 (cucurbitacin I), a selective Janus kinase/signal transducer and activator of transcription 3 signaling pathway inhibitor with potent antitumor activity against human and murine cancer cells in mice. Cancer Res 63:1270-1279.

94 Kaplan DH, Shankaran V, Dighe AS*, et al.* (1998). Demonstration of an interferon gamma-dependent tumor surveillance system in immunocompetent mice. Proc Natl Acad Sci U S A 95:7556-7561.

95 Kortylewski M WT, Wei S, Zhang S, Pilon-Thomas S, Lutz L, Kay H, Ghansah T, Nguyen K, Kerr WG, Mule J, Jove R, Pardoll D, Yu H. (2004). Stat-3 signaling in the hematopoetic system regulates tumor immune surveillance. *submitted*